Supporting information for

A Stable and Biocompatible Shortwave Infrared Nanoribbon for Dual-channel in vivo Imaging

Cheng Yao[1,2], Ruwei Wei[1,2], Xiao Luo[3], Jie Zhou[4,5], Xiaodong Zhang[1,2], Xicun Lu[1,2], Yan Dong[1,2], Ruofan Chu[1,2], Yuxin Sun[1,2], Yu Wang[3], Wencheng Xia[6], Dahui Qu[1], Cong Liu[6], Jun Ren[7,8], Guangbo Ge[9], Jinquan Chen[4,5], Xuhong Qian[1,2,3], Youjun Yang[1,2,*]

1. State Key Laboratory of Bioreactor Engineering, East China University of Science and Technology, Shanghai 200237, China
2. Shanghai Key Laboratory of Chemical Biology, Shanghai Frontiers Science Center of Optogenetic Techniques for Cell Metabolism, School of Pharmacy, East China University of Science and Technology, Shanghai 200237, China
3. Shanghai Engineering Research Center of Molecular Therapeutics and New Drug Development, School of Chemistry and Molecular Engineering, East China Normal University, Shanghai 200241, China
4. State Key Laboratory of Precision Spectroscopy, East China Normal University, Shanghai 200241, China
5. School of Physics and Electronic Science, East China Normal University, Shanghai 200241, China
6. Interdisciplinary Research Center on Biology and Chemistry, Shanghai Institute of Organic Chemistry, Chinese Academy of Sciences, Shanghai, 201210, China
7. Hubei Key Laboratory for Precision Synthesis of Small Molecule Pharmaceuticals & Ministry of Education Key Laboratory for the Synthesis and Application of Organic Functional Molecules, Hubei University, Wuhan 430062, China
8. Hubei Key Laboratory for Precision Synthesis of Small Molecule Pharmaceuticals & Ministry of Education Key Laboratory for the Synthesis and Application of Organic Functional Molecules, Hubei University, Wuhan 430062, China
9. Institute of Interdisciplinary Integrative Medicine Research, Shanghai University of Traditional Chinese Medicine, Cailun Road 1200, Shanghai 201203, China

Contact: youjunyang@ecust.edu.cn.

Table of contents

Page	Content	
S3	Supplementary Fig. 1	Energy splitting diagram.
S3	Supplementary Fig. 2	The detailed packing mode
S4	Supplementary Fig. 3	Electrostatic potential distribution calculations.
S4-7	Supplementary Fig. 4-11	The absorption and fluorescence emission spectra of water-soluble ESi5 analogues in organic solvent.
S7	Supplementary Fig. 12-13	NaCl-concentration-dependent spectral changes of **ESi5-NS** and **ESi5-N**.
S8	Supplementary Tab. 1	Photophysical parameters of water-soluble ESi5 analogues.
S9	Supplementary Fig. 14	Concentration-dependent spectral changes of **ESi5-NS** and **ESi5-N** in PBS.
S9	Supplementary Fig. 15	Spectral changes after thermal annealing of JV-aggregates.
S10-12	Supplementary Fig. 16-21	Spectral deconvolution of JV-aggregates.
S13	Supplementary Tab. 2	Spectral deconvolution parameters of JV-aggregates.
S13	Supplementary Fig. 22	The absorption spectrum of **ESi5-S agg** in PBS (10% FBS)
S14-16	Supplementary Fig. 23-30	Electron microscopy characterization.
S16	Supplementary Fig. 31	Femtosecond transient absorption (fs-TA) spectra of **ESi5-S agg**.
S17-19	Supplementary Fig. 32-35	Stability of **ESi5-S agg**.
S18	Supplementary Table 3	The photobleaching rates and the bleaching half-life ($\tau_{1/2}$).
S20-21	Supplementary Fig. 36-37	Temperature-dependent stability of JV-aggregates.
S21-22	Supplementary Fig. 38-39	The cytotoxicity test and the hemolysis test.
S22-24	Supplementary Fig. 40-44	The dual-channel fluorescence imaging.
S25	Supplementary Fig. 45-46	*In vivo* toxicity study
S26	Supplementary Fig. 47	*In vitro* calcium-binding experiments.
S26-31	Supplementary Fig. 48-57	The synthetic scheme of water-soluble ESi5 analogues.
S31-S43	Supplementary Fig. 58-71	The ^{1}H-/^{13}C-NMR and HRMS spectra.
S44	Supplementary Fig. 82-83	The ORTEP-style illustration of **ESi5•Cl^{-}** and **ESi5•PF$_6^{-}$**

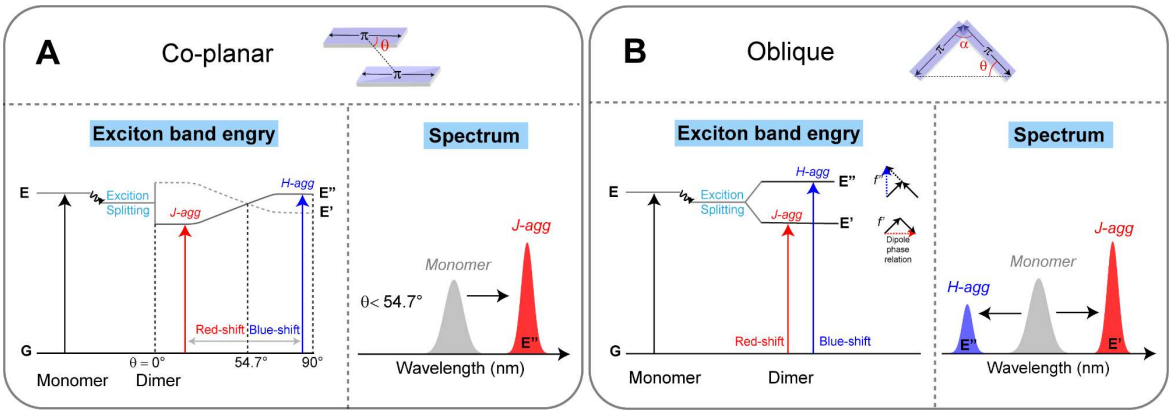

Supplementary Fig. 1: Energy splitting diagram of (A) linearly coupled H-dimer or J-dimer, and (B) non-linearly coupled oblique-dimer.

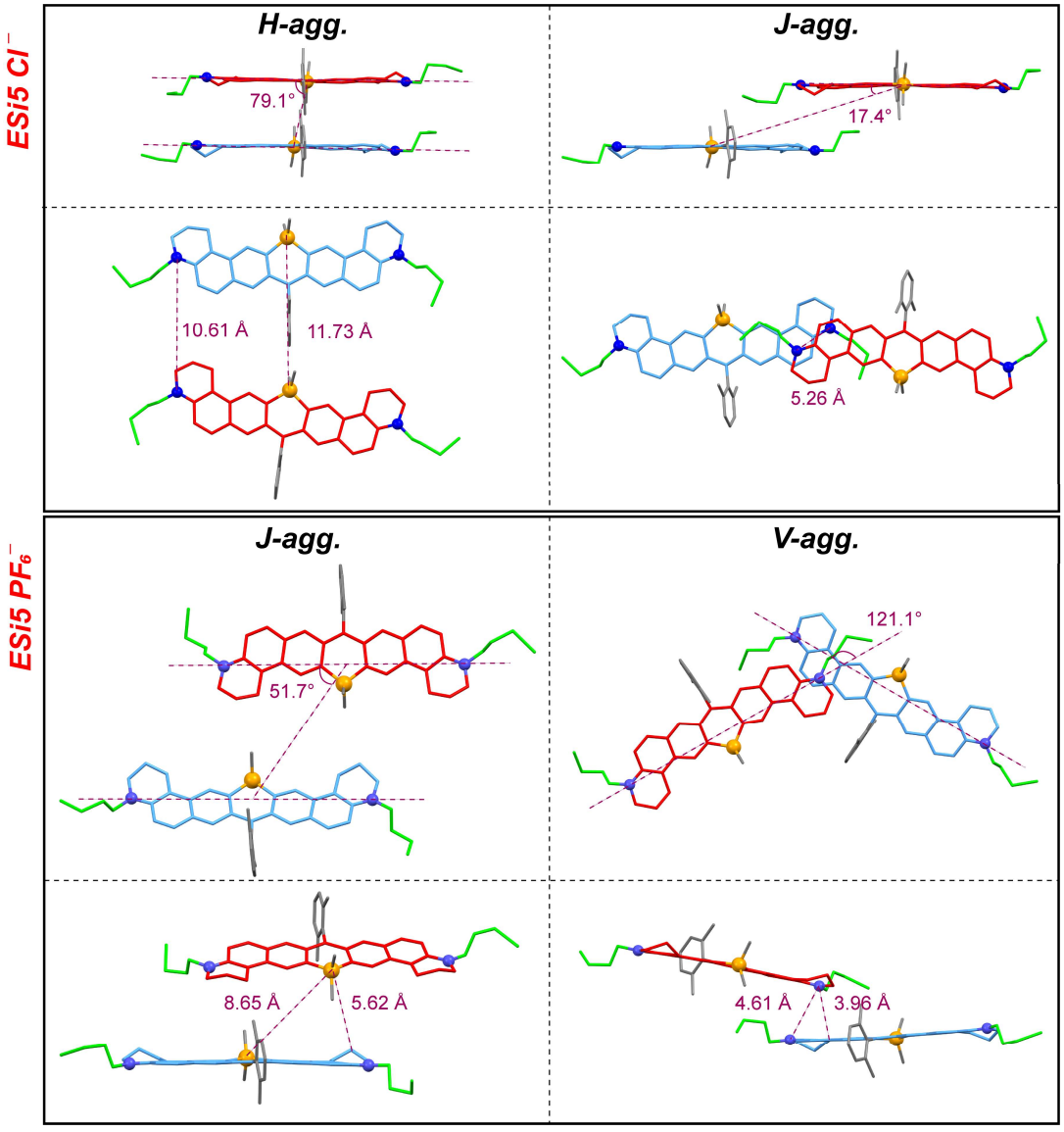

Supplementary Fig. 2: The detailed packing mode of **ESi5•Cl**$^{-}$ (H-aggregate and J-aggregate) and **ESi5•PF6**$^{-}$ (J-aggregate and V-aggregate). Including slipping angle and interatomic distance.

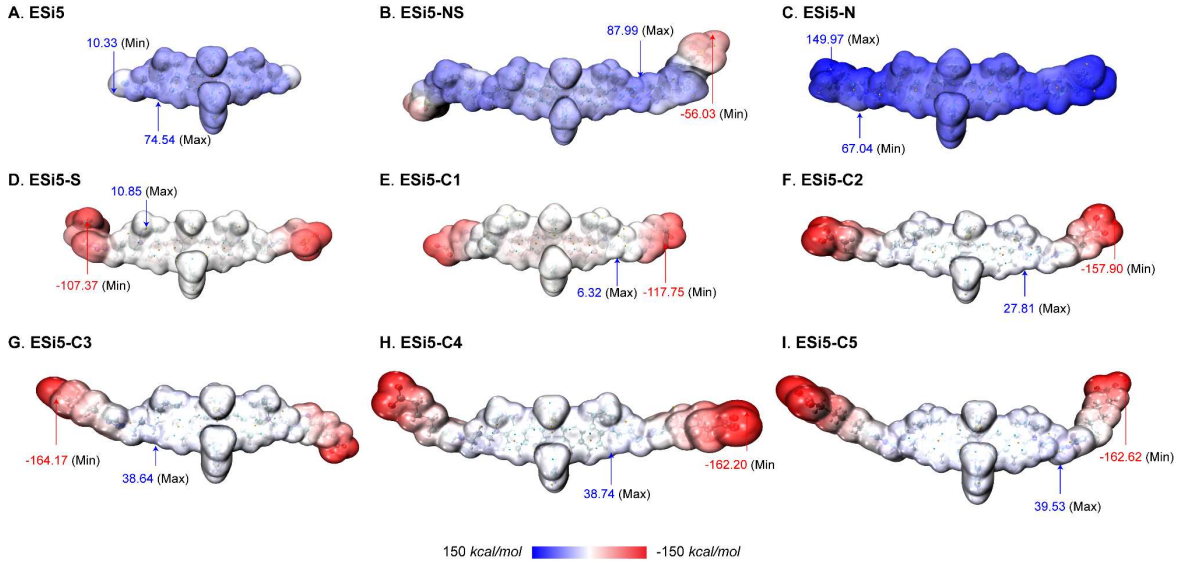

Supplementary Fig. 3: Electrostatic potential (ESP) surface of **ESi5**, **ESi5-NS**, **ESi5-N**, **ESi5-S** and **ESi5-C1**(-**C5**) calculated at B3LYP/6-31G level.

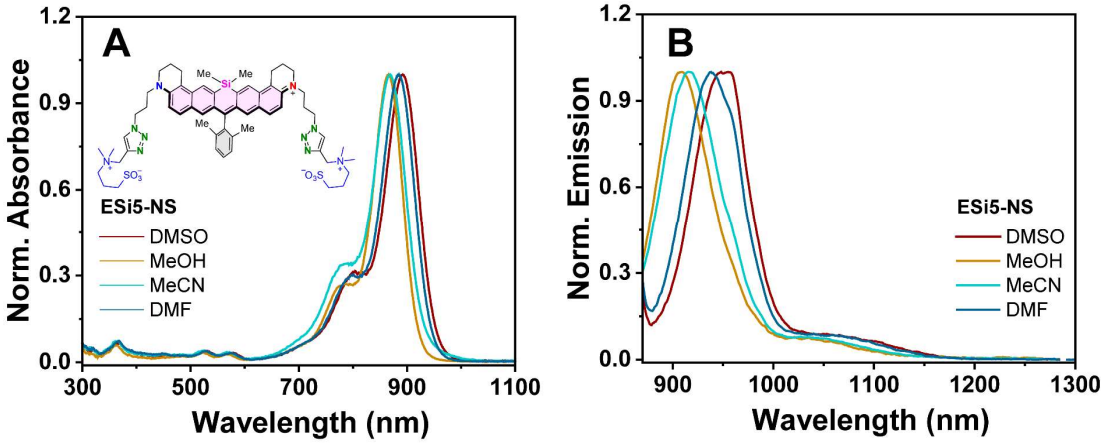

Supplementary Fig. 4: The normalized UV-Vis absorption (A) and fluorescence emission (B) spectra of **ESi5-NS** in different organic solvents, *i.e.* DMSO, MeOH, MeCN, and DMF. Inset: the chemical structure of **ESi5-NS**.

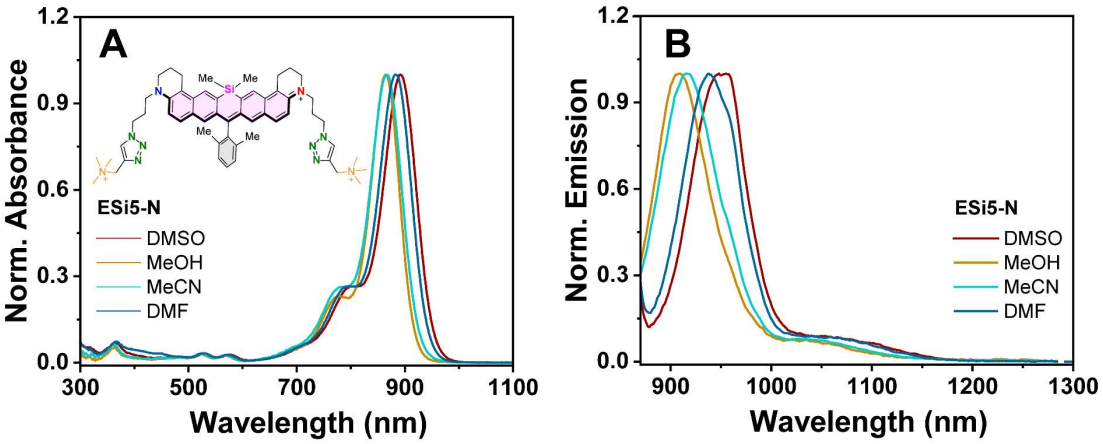

Supplementary Fig. 5: The normalized UV-Vis absorption (A) and fluorescence emission (B) spectra of **ESi5-N** in different organic solvents, *i.e.* DMSO, MeOH, MeCN, and DMF. Inset: the chemical structure of **ESi5-N**.

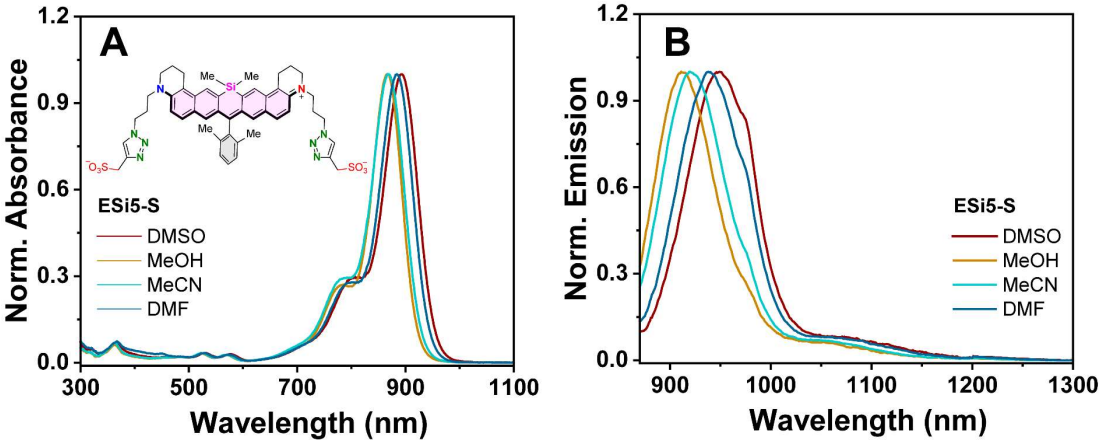

Supplementary Fig. 6: The normalized UV-Vis absorption (A) and fluorescence emission (B) spectra of **ESi5-S** in different organic solvents, *i.e.* DMSO, MeOH, MeCN, and DMF. Inset: the chemical structure of **ESi5-S**.

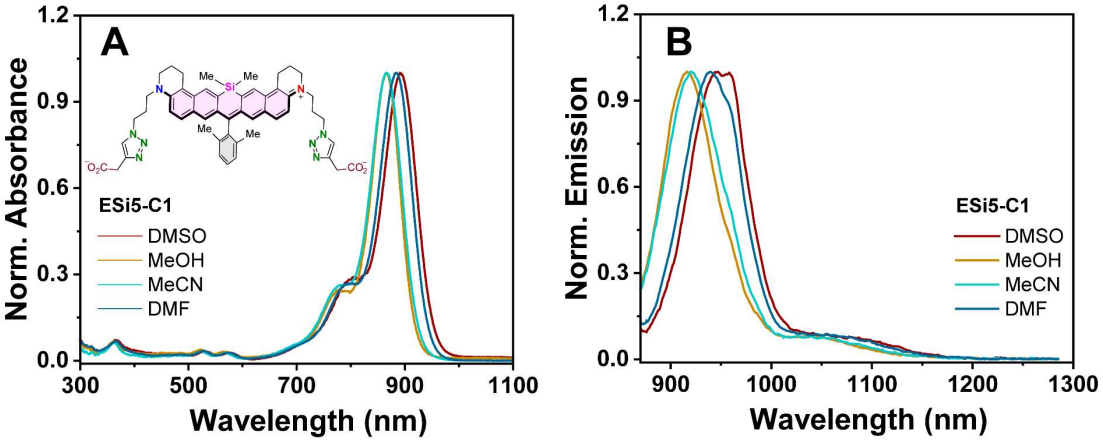

Supplementary Fig. 7: The normalized UV-Vis absorption (A) and fluorescence emission (B) spectra of **ESi5-C1** in different organic solvents, *i.e.* DMSO, MeOH, MeCN, and DMF. Inset: the chemical structure of **ESi5-C1**.

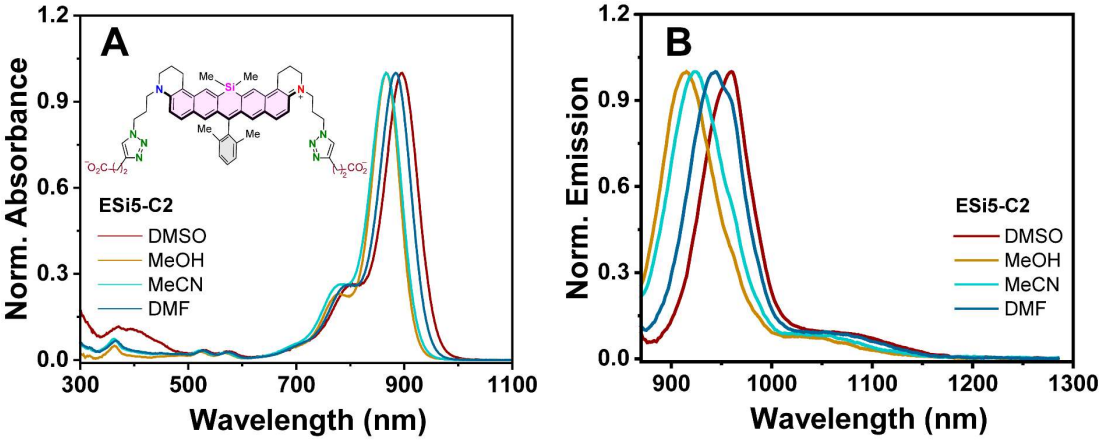

Supplementary Fig. 8: The normalized UV-Vis absorption (A) and fluorescence emission (B) spectra of **ESi5-C2** in different organic solvents, *i.e.* DMSO, MeOH, MeCN, and DMF. Inset: the chemical structure of **ESi5-C2**.

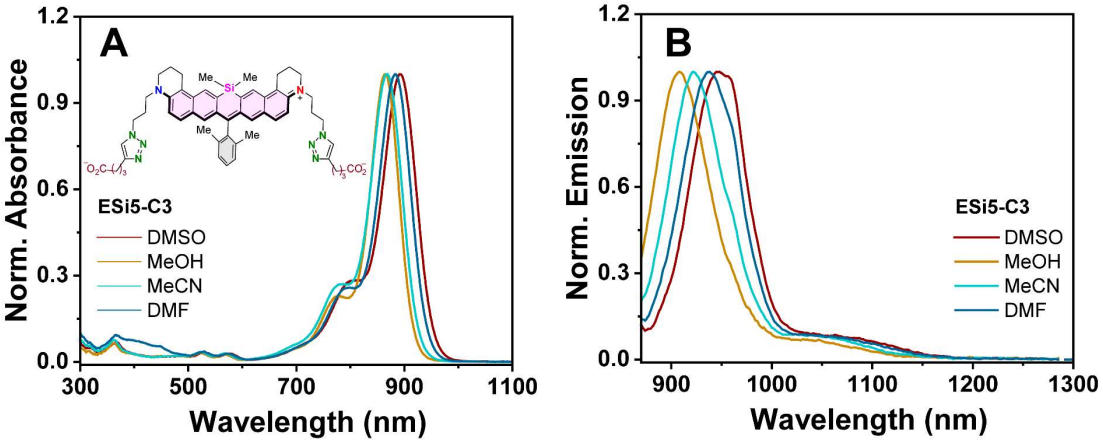

Supplementary Fig. 9: The normalized UV-Vis absorption (A) and fluorescence emission (B) spectra of **ESi5-C3** in different organic solvents, *i.e.* DMSO, MeOH, MeCN, and DMF. Inset: the chemical structure of **ESi5-C3**.

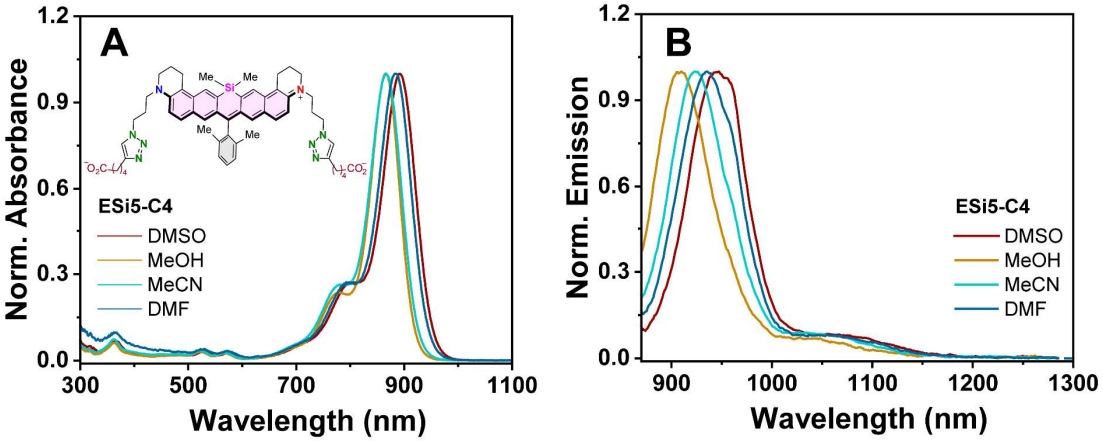

Supplementary Fig. 10: The normalized UV-Vis absorption (A) and fluorescence emission (B) spectra of **ESi5-C4** in different organic solvents, *i.e.* DMSO, MeOH, MeCN, and DMF. Inset: the chemical structure of **ESi5-C4**.

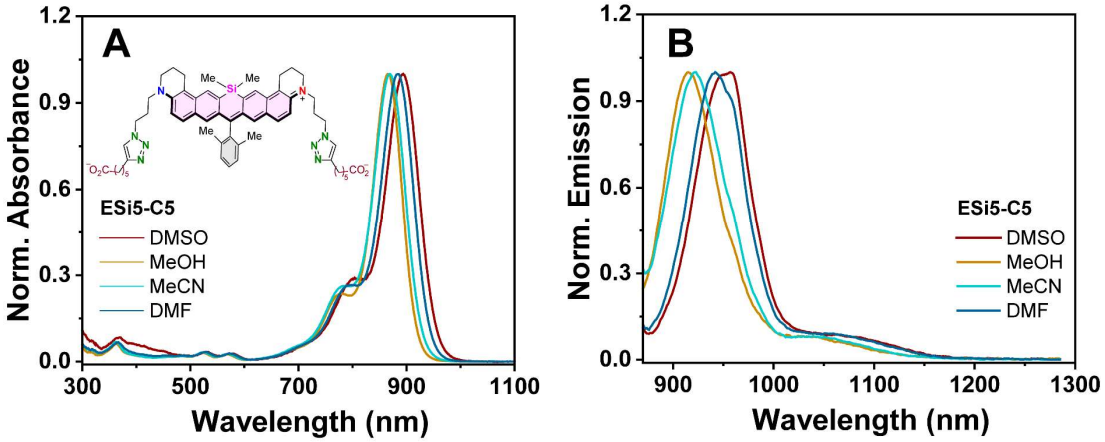

Supplementary Fig. 11: The normalized UV-Vis absorption (A) and fluorescence emission (B) spectra of **ESi5-C5** in different organic solvents, *i.e.* DMSO, MeOH, MeCN, and DMF. Inset: the chemical structure of **ESi5-C5.**

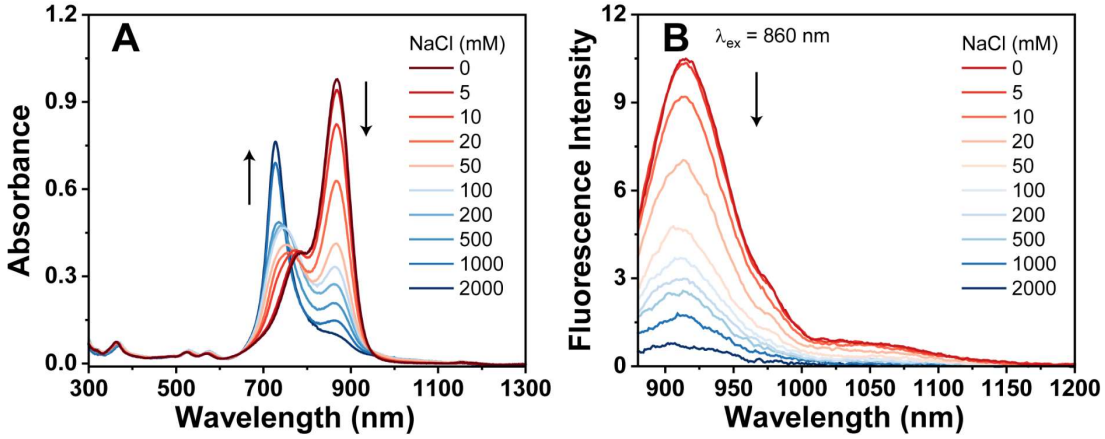

Supplementary Fig. 12: The changes of the (A) absorption and (B) fluorescence spectra of **ESi5-NS** in water with respect to the NaCl concentration. (λ_{ex} = 860 nm).

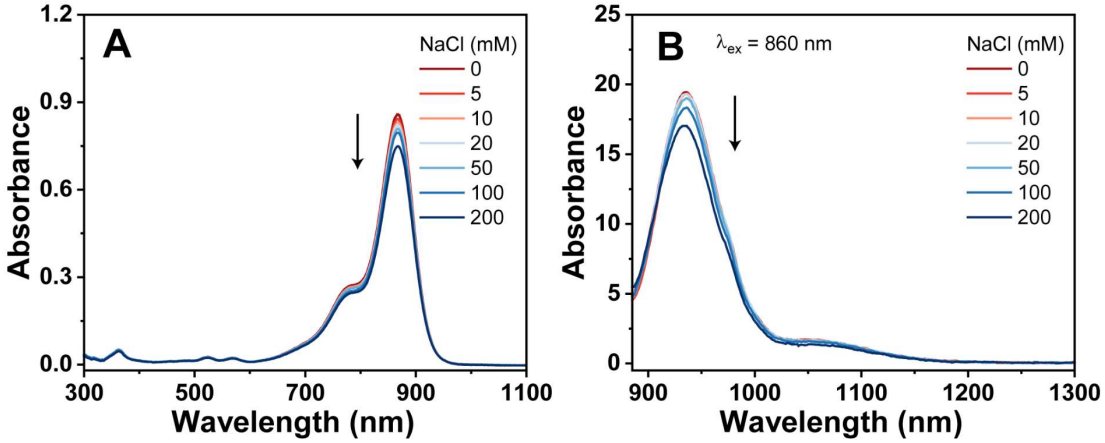

Supplementary Fig. 13:. The changes of the (A) absorption and (B) fluorescence spectra of **ESi5-N** in water with respect to the NaCl concentration. (λ_{ex} = 860 nm).

Supplementary Table 1: Photophysical parameters of water-soluble ESi5 analogues in different organic solvents, *i.e.* DMSO, MeOH, MeCN, and DMF.

Dye	Solvent	λ_{abs} (nm)	ε ($\times 10^5$ cm^{-1} M^{-1})	λ_{em} (nm)	ϕ (%)	Stokes Shift (nm)	Brightness (M^{-1} cm^{-1})
ESi5-NS	DMSO	892	1.06	946	9.4	54	9964
	MeOH	866	1.00	916	5.4	50	5400
	MeCN	869	1.01	922	7.3	53	7373
	DMF	885	0.75	938	7.3	53	5775
ESi5-N	DMSO	892	1.03	955	8	63	8240
	MeOH	865	1.16	909	5.5	44	6380
	MeCN	865	1.16	916	4.8	51	5568
	DMF	882	0.40	938	4.8	56	4800
ESi5-S	DMSO	893	2.35	949	6.3	56	8505
	MeOH	868	1.35	911	4.1	43	5535
	MeCN	869	1.32	920	8.8	51	11616
	DMF	885	1.23	938	8.8	53	9594
ESi5-C1	DMSO	891	1.23	947	8.9	56	10578
	MeOH	866	1.58	916	5.2	50	8216
	MeCN	865	0.92	920	9.2	56	8464
	DMF	883	0.64	939	9.2	56	3712
ESi5-C2	DMSO	896	1.23	960	8.9	64	10947
	MeOH	867	1.48	915	5.0	48	7400
	MeCN	866	1.01	924	6.0	58	6060
	DMF	884	1.23	944	8.6	60	10578
ESi5-C3	DMSO	892	0.88	956	8.6	64	7568
	MeOH	865	1.42	908	6.0	43	8520
	MeCN	869	1.27	922	9.0	53	11430
	DMF	884	0.77	938	9.0	54	6160
ESi5-C4	DMSO	894	0.89	957	9.4	63	8366
	MeOH	865	1.36	915	4.9	50	6664
	MeCN	868	0.96	922	6.3	54	6048
	DMF	885	0.32	942	6.3	57	1824
ESi5-C5	DMSO	894	0.89	957	9.4	63	8366
	MeOH	865	1.36	915	4.9	50	6664
	MeCN	868	0.96	922	6.3	54	6048
	DMF	885	0.32	942	6.3	57	1824

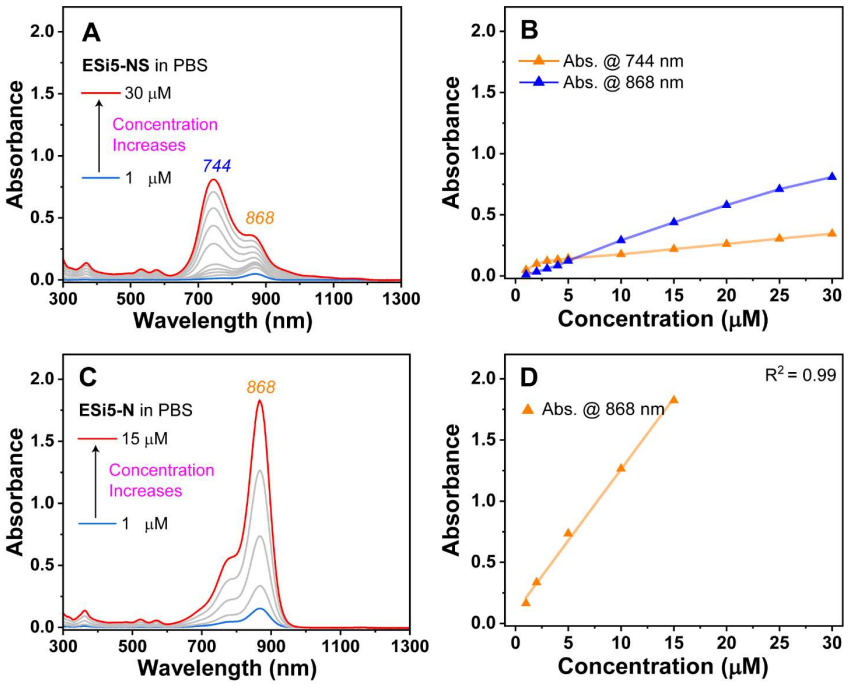

Supplementary Fig. 14: Concentration-dependent absorption spectra of **ESi5-NS** (A), **ESi5-N** (C) and **ESi5-S** (E) in PBS (pH = 7.4, 10 mM, containing MeOH < 2%) at room temperature. Plot of absorbance versus concentration at specific wavelengths of **ESi5-NS** (B), **ESi5-N** (D) and **ESi5-S** (F).

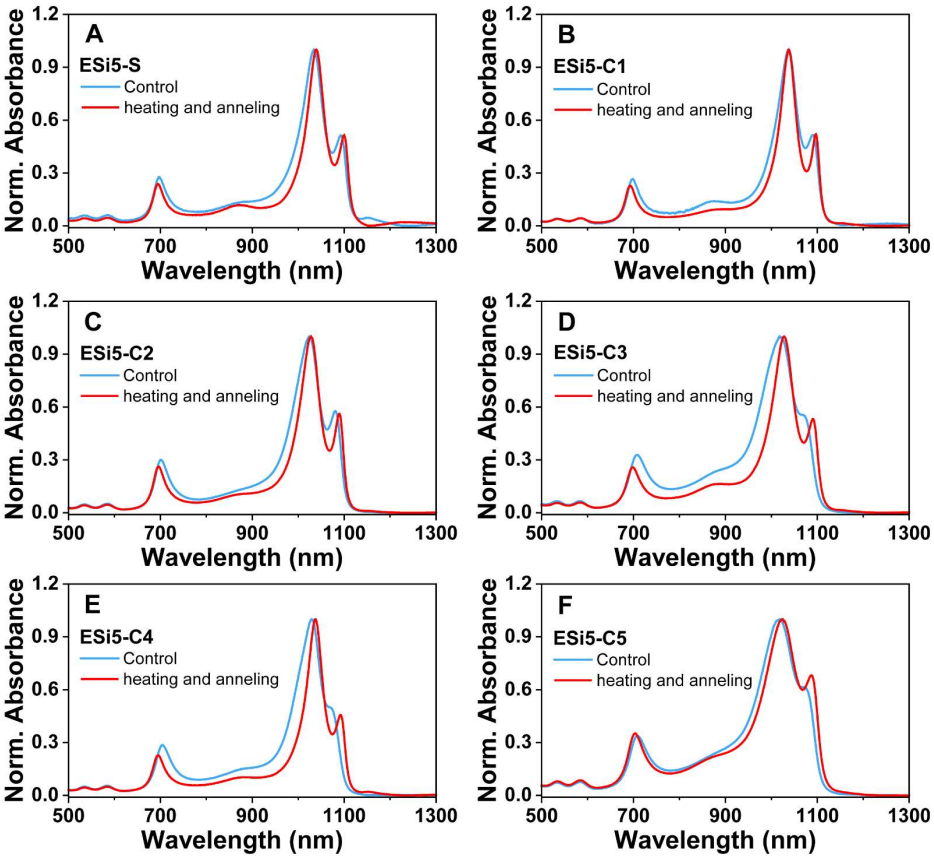

Supplementary Fig. 15: The Normalized absorption spectra of **ESi5-S**, **ESi5-C1**(**-C5**) in PBS (pH =7.4, 10 mM) (blue line) and after thermal annealing (red line).

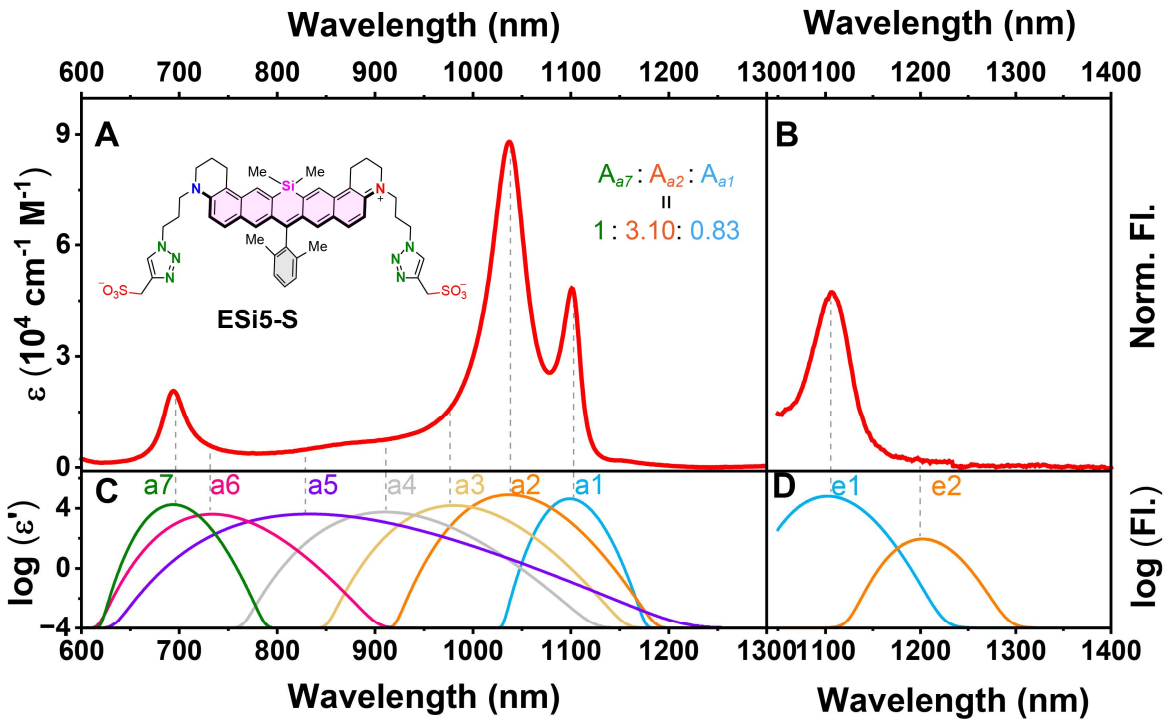

Supplementary Fig. 16: The absorption (A) and fluorescence emission (B) spectra of the heating/annealing-treated **ESi5-S agg** in PBS (pH =7.4, 10 mM). And the absorption and emission were deconvoluted into seven (C) and two (D) constituting peaks, respectively.

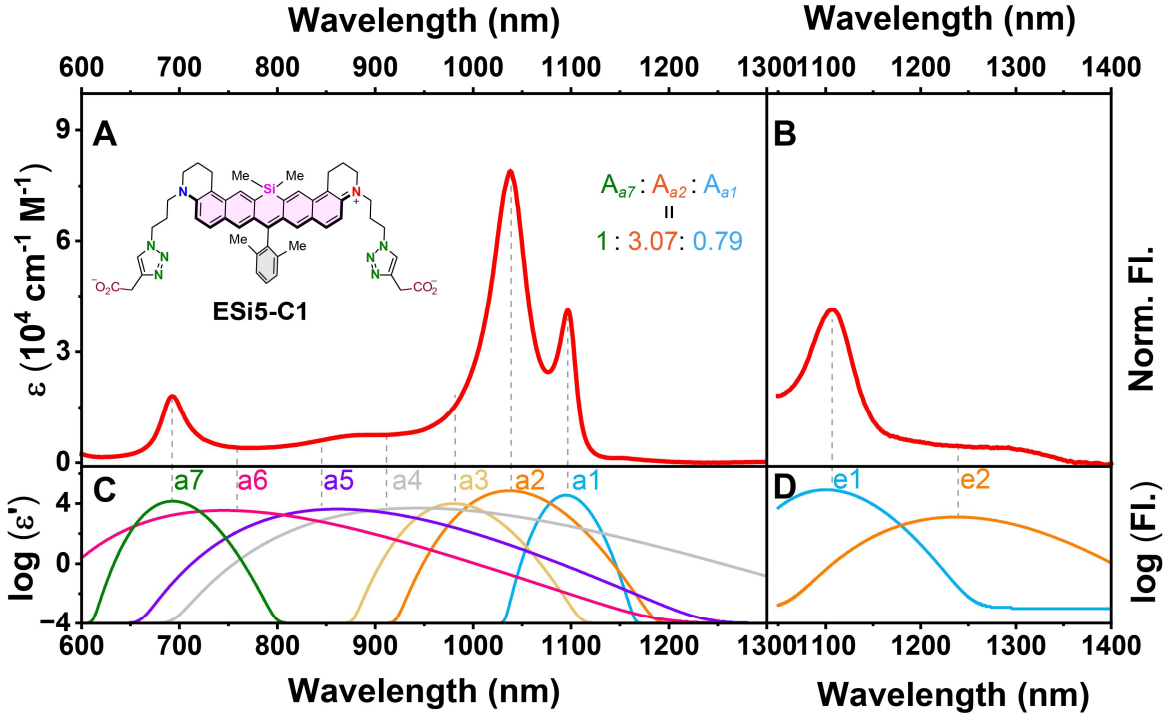

Supplementary Fig. 17: The absorption (A) and fluorescence emission (B) spectra of the heating/annealing-treated **ESi5-C1 agg** in PBS (pH =7.4, 10 mM). And the absorption and emission were deconvoluted into seven (C) and two (D) constituting peaks, respectively.

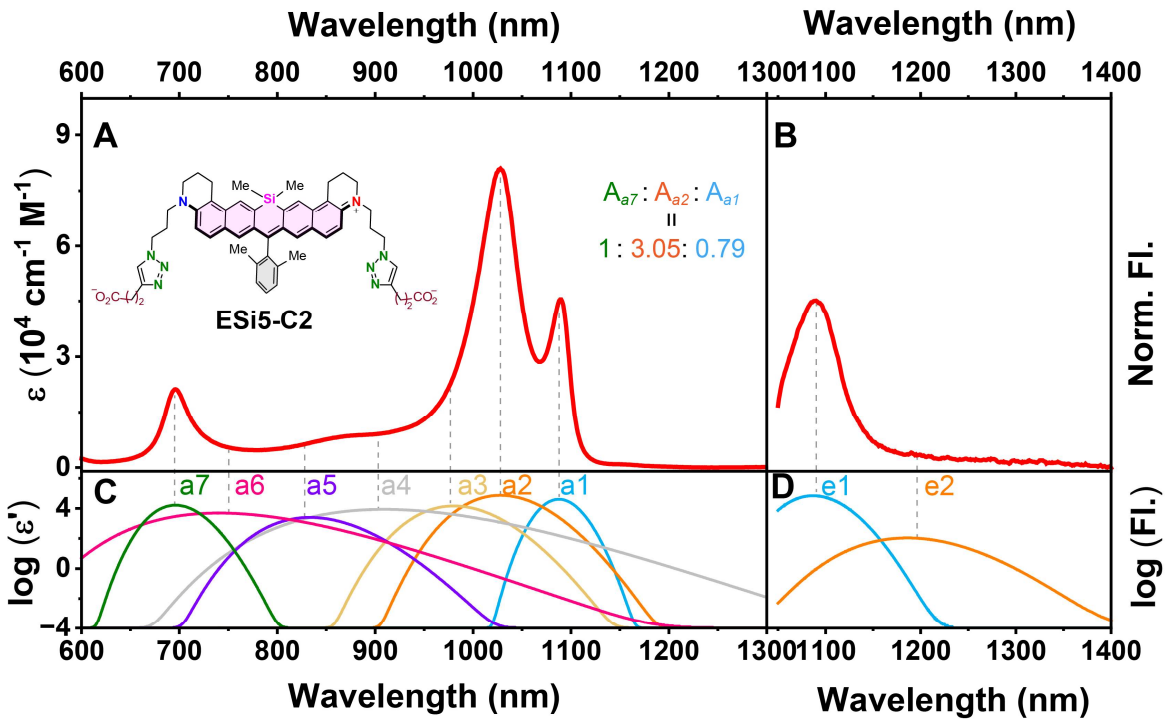

Supplementary Fig. 18: The absorption (A) and fluorescence emission (B) spectra of the heating/annealing-treated **ESi5-C2 agg** in PBS (pH =7.4, 10 mM). And the absorption and emission were deconvoluted into seven (C) and two (D) constituting peaks, respectively.

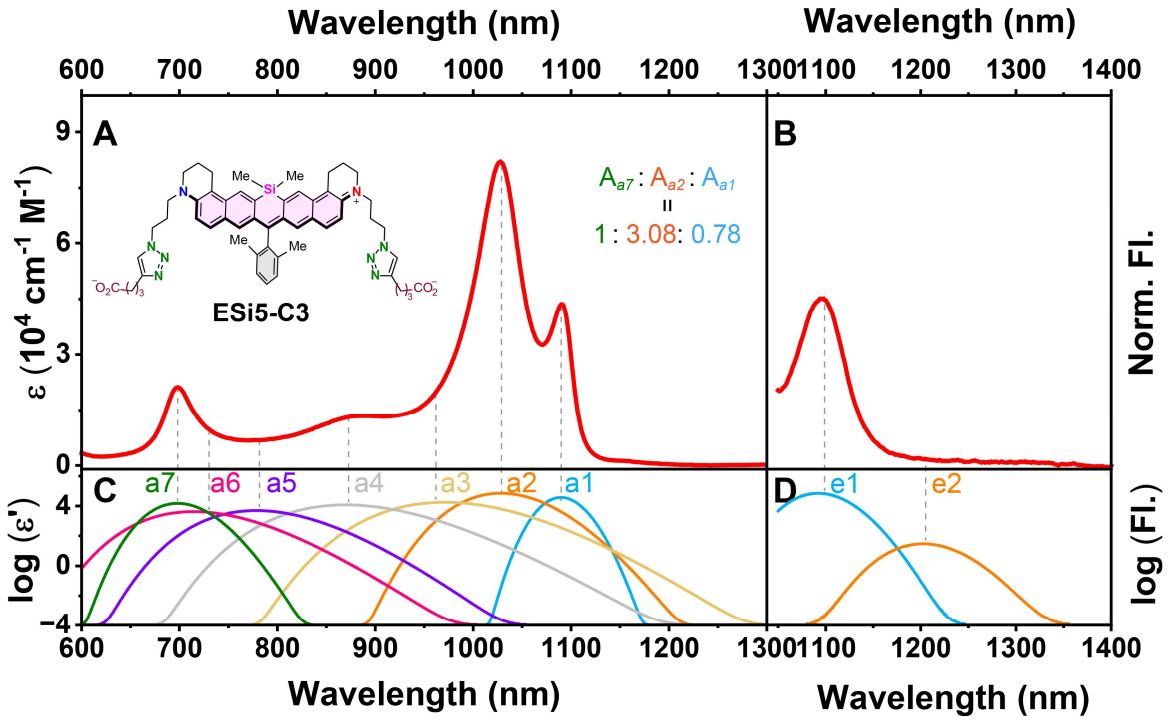

Supplementary Fig. 19: The absorption (A) and fluorescence emission (B) spectra of the heating/annealing-treated **ESi5-C3 agg** in PBS (pH =7.4, 10 mM). And the absorption and emission were deconvoluted into seven (C) and two (D) constituting peaks, respectively.

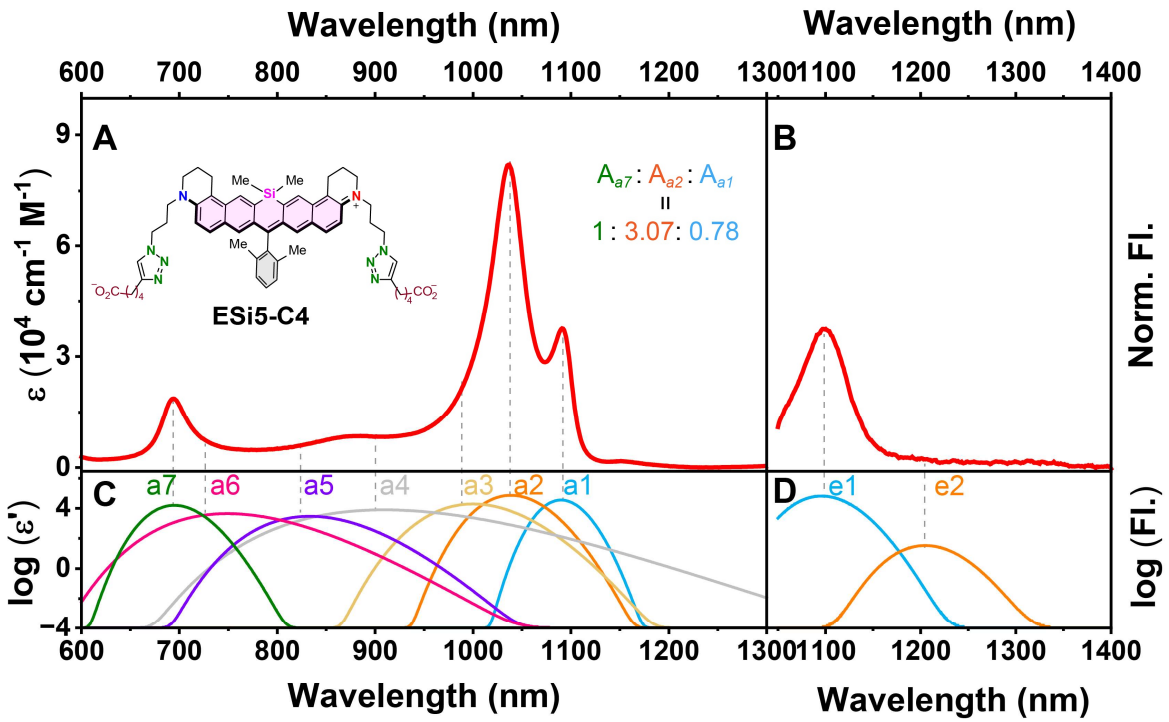

Supplementary Fig. 20: The absorption (A) and fluorescence emission (B) spectra of the heating/annealing-treated **ESi5-C4 agg** in PBS (pH =7.4, 10 mM). And the absorption and emission were deconvoluted into seven (C) and two (D) constituting peaks, respectively.

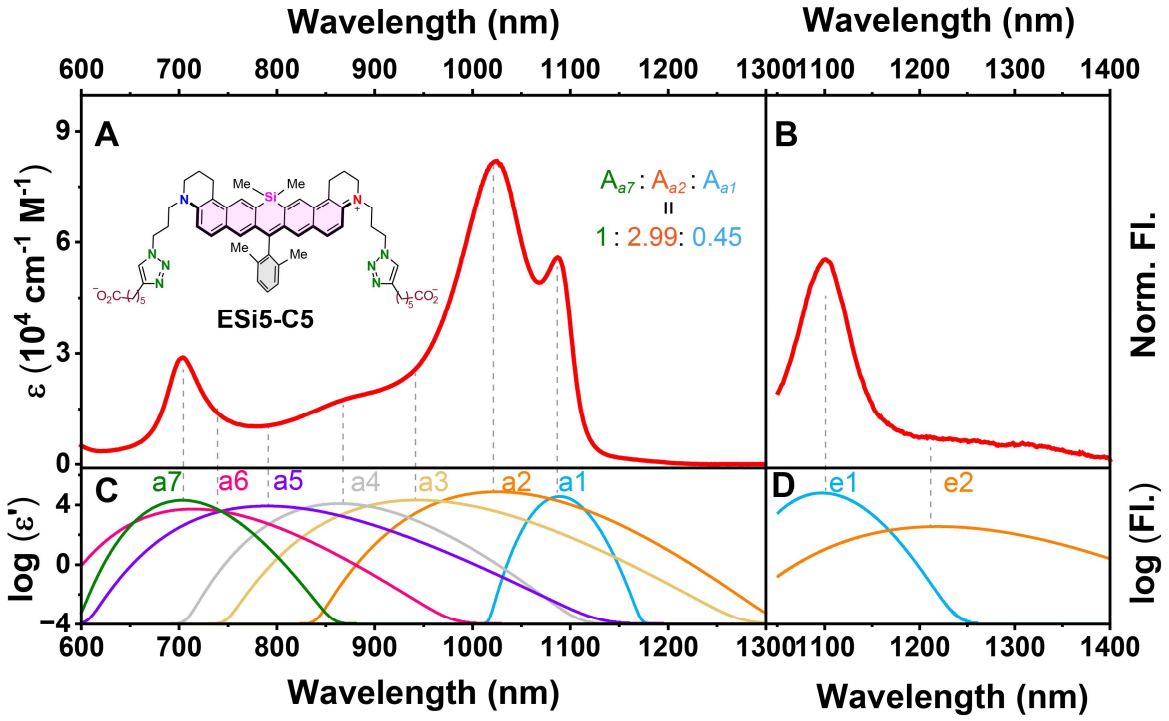

Supplementary Fig. 21: The absorption (A) and fluorescence emission (B) spectra of the heating/annealing-treated **ESi5-C5 agg** in PBS (pH =7.4, 10 mM). The absorption and emission were deconvoluted into seven (C) and two (D) constituting peaks, respectively.

Supplementary Table 2: The spectral deconvolution parameters of heating/annealing-treated **ESi5-S** and **ESi5-C1**(**-C5**) **agg** in PBS (pH =7.4, 10 mM).

Dye	Peak	Wavelength (nm)	FWHM (cm^{-1})	Area (10^7 L mol^{-1} cm^{-2})
ESi5-S	a1	1099	224.8	1.03
	a2	1037	448.3	3.85
	a7	694	657.4	1.24
ESi5-C1	a1	1094	216.2	0.84
	a2	1038	420.7	3.25
	a7	692	692.9	1.06
ESi5-C2	a1	1088	229.3	1.00
	a2	1028	483.3	3.84
	a7	696	721.0	1.26
ESi5-C3	a1	1089	254.5	1.03
	a2	1028	512.8	4.09
	a7	697	817.8	1.33
ESi5-C4	a1	1090	232.0	0.88
	a2	1037	413.0	3.47
	a7	695	715.8	1.13
ESi5-C5	a1	1089	245.5	0.96
	a2	1025	790.2	6.34
	a7	703	973.6	2.12

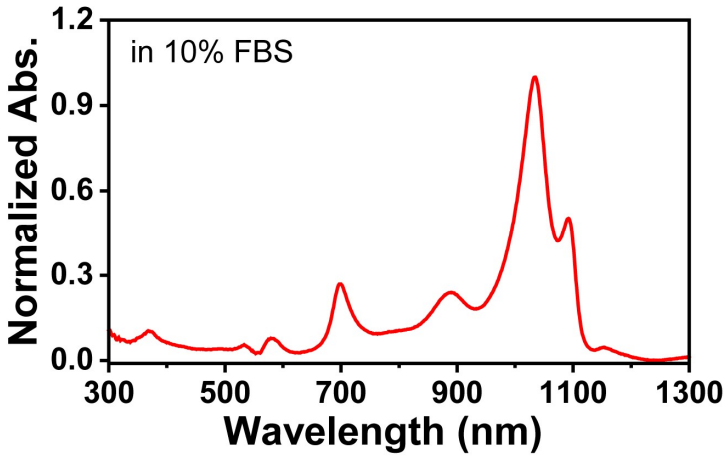

Supplementary Fig. 22: The absorption spectrum of **ESi5-S agg** in PBS (5 μM), containing 10% FBS.

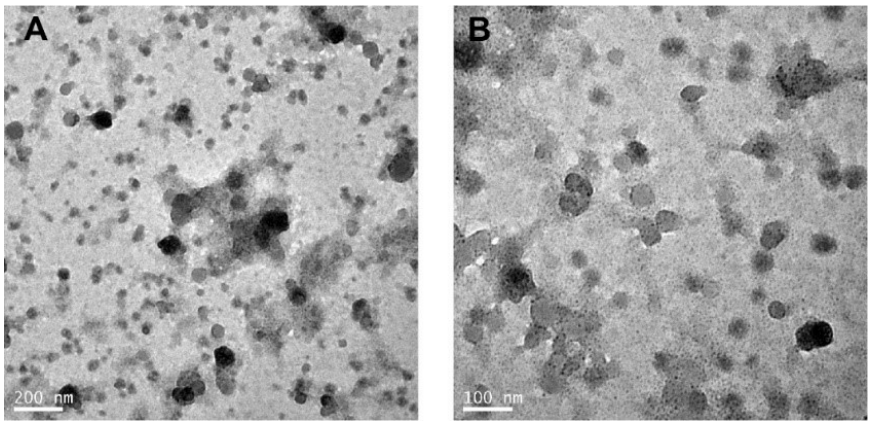

Supplementary Fig. 23: (A, B) The TEM images of **ESi5-NS agg** (200 μM) in PBS (pH = 7.4, 10 mM). Scale bar =200 nm and 100 nm, respectively.

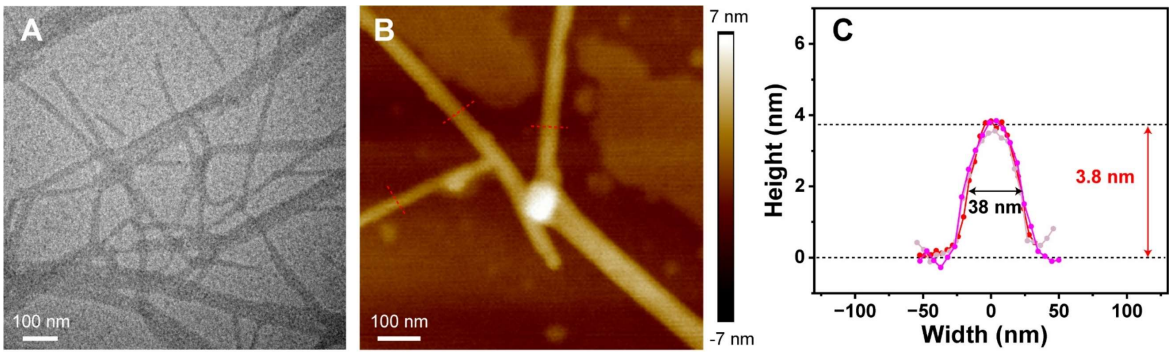

Supplementary Fig. 24: (A) The TEM image of **ESi5-C1 agg** (200 μM) in deionized water (containing 4% methanol). (B, C) The AFM image of **ESi5-C1 agg** (200 μM) with cross-section height analyses along red dash lines. Scale bar = 100 nm.

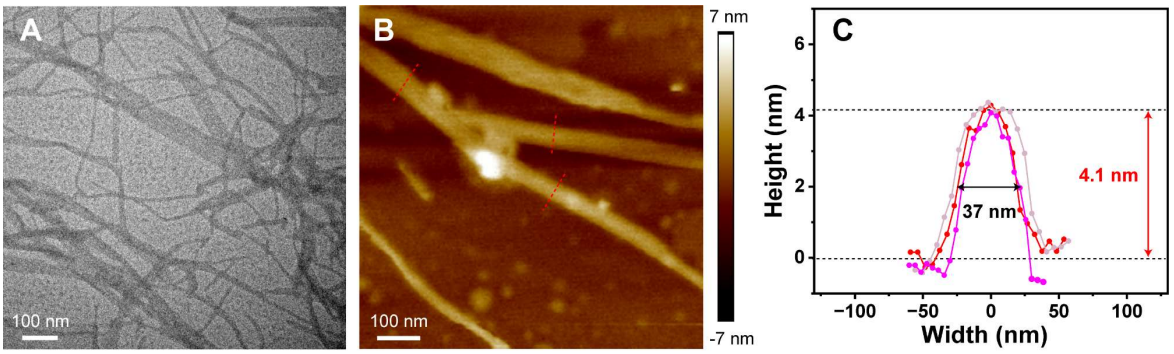

Supplementary Fig. 25: (A) The TEM image of **ESi5-C2 agg** (200 μM) in deionized water (containing 4% methanol). (B, C) The AFM image of **ESi5-C2 agg** (200 μM) with cross-section height analyses along red dash lines. Scale bar = 100 nm.

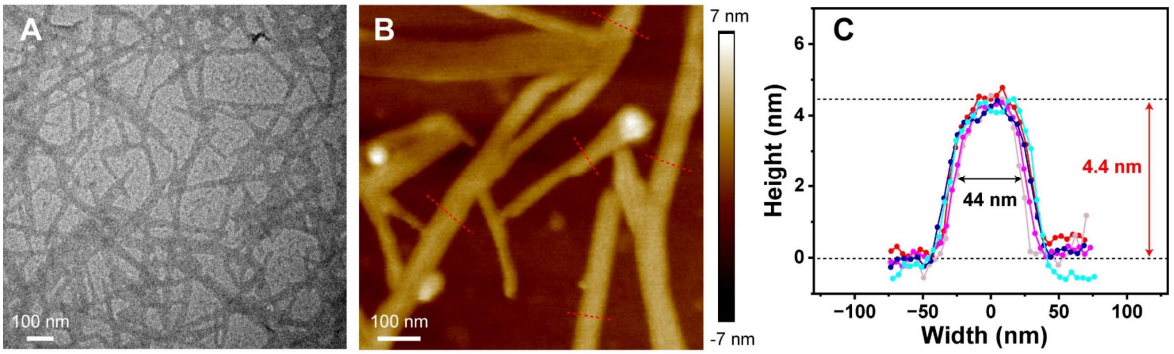

Supplementary Fig. 26: (A) The TEM image of **ESi5-C3 agg** (200 μM) in deionized water (containing 4% methanol). (B, C) The AFM image of **ESi5-C3 agg** (200 μM) with cross-section height analyses along red dash lines. Scale bar = 100 nm.

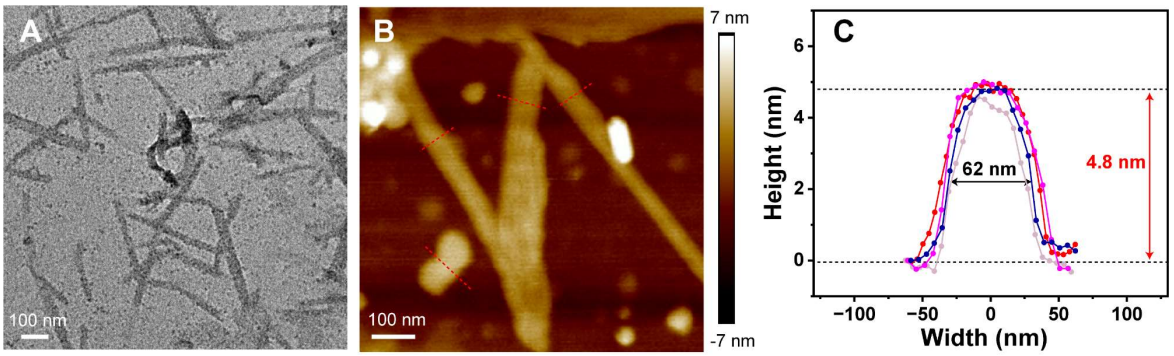

Supplementary Fig. 27: (A) The TEM image of **ESi5-C4 agg** (200 μM) in deionized water (containing 4% methanol). (B, C) The AFM image of **ESi5-C4 agg** (200 μM) with cross-section height analyses along red dash lines. Scale bar = 100 nm.

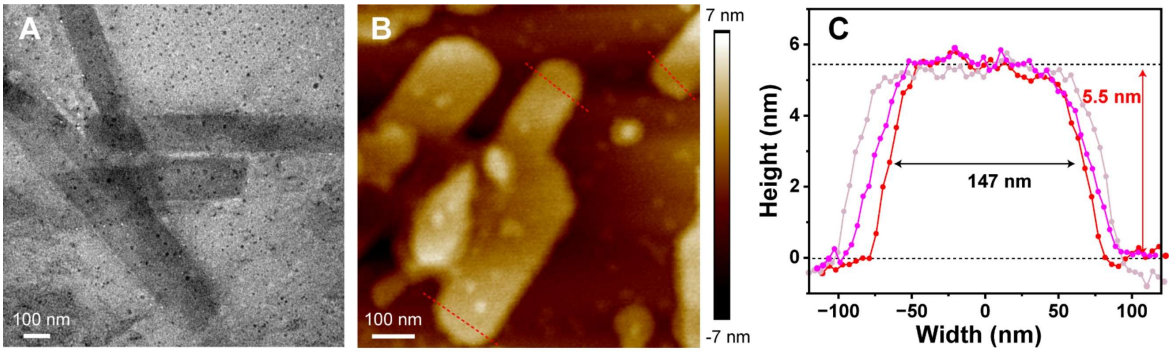

Supplementary Fig. 28: (A) The TEM image of **ESi5-C5 agg** (200 μM) in deionized water (containing 4% methanol). (B, C) The AFM image of **ESi5-C5 agg** (200 μM) with cross-section height analyses along red dash lines. Scale bar = 100 nm.

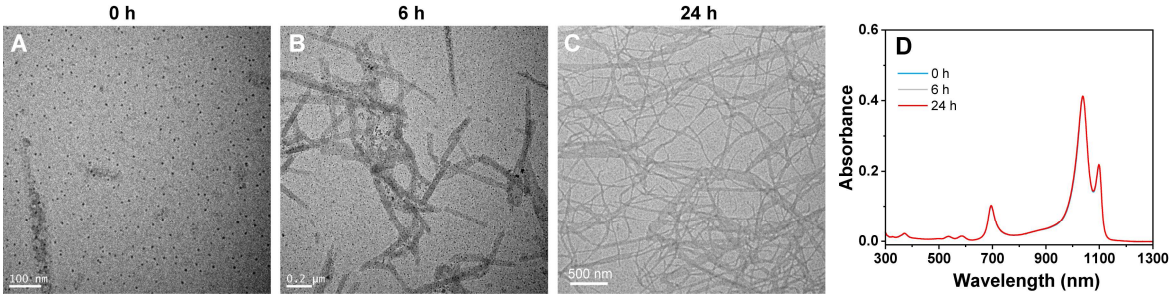

Supplementary Fig. 29: (A, B, C) The TEM images and (D) absorbance spectrum of **ESi5-S agg** (200 μM in H_2O, containing 4% MeOH) self-assembled for 0 h, 6 h and 24 h, respectively.

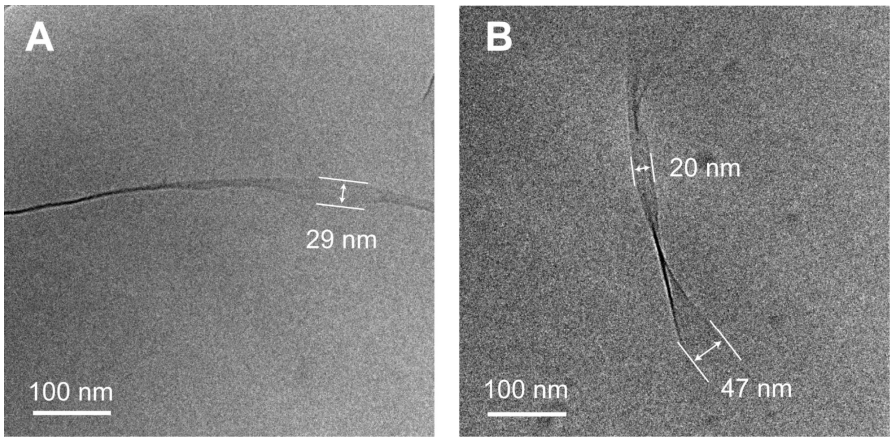

Supplementary Fig. 30: (A, B) The Cryo-EM images of **ESi5-S agg** (200 μM) in deionized H_2O (containing 4% methanol). Scale bar = 100 nm.

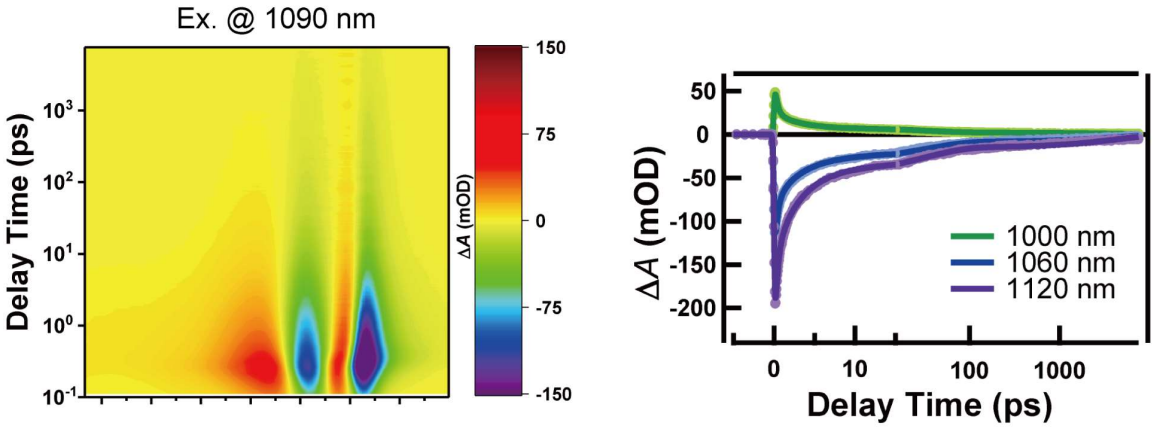

Supplementary Fig. 31: Femtosecond transient absorption (fs-TA) spectra of **ESi5-S agg** (10 μM) in PBS (pH = 7.4, 10 mM) (λ_{pump} = 1090 nm)

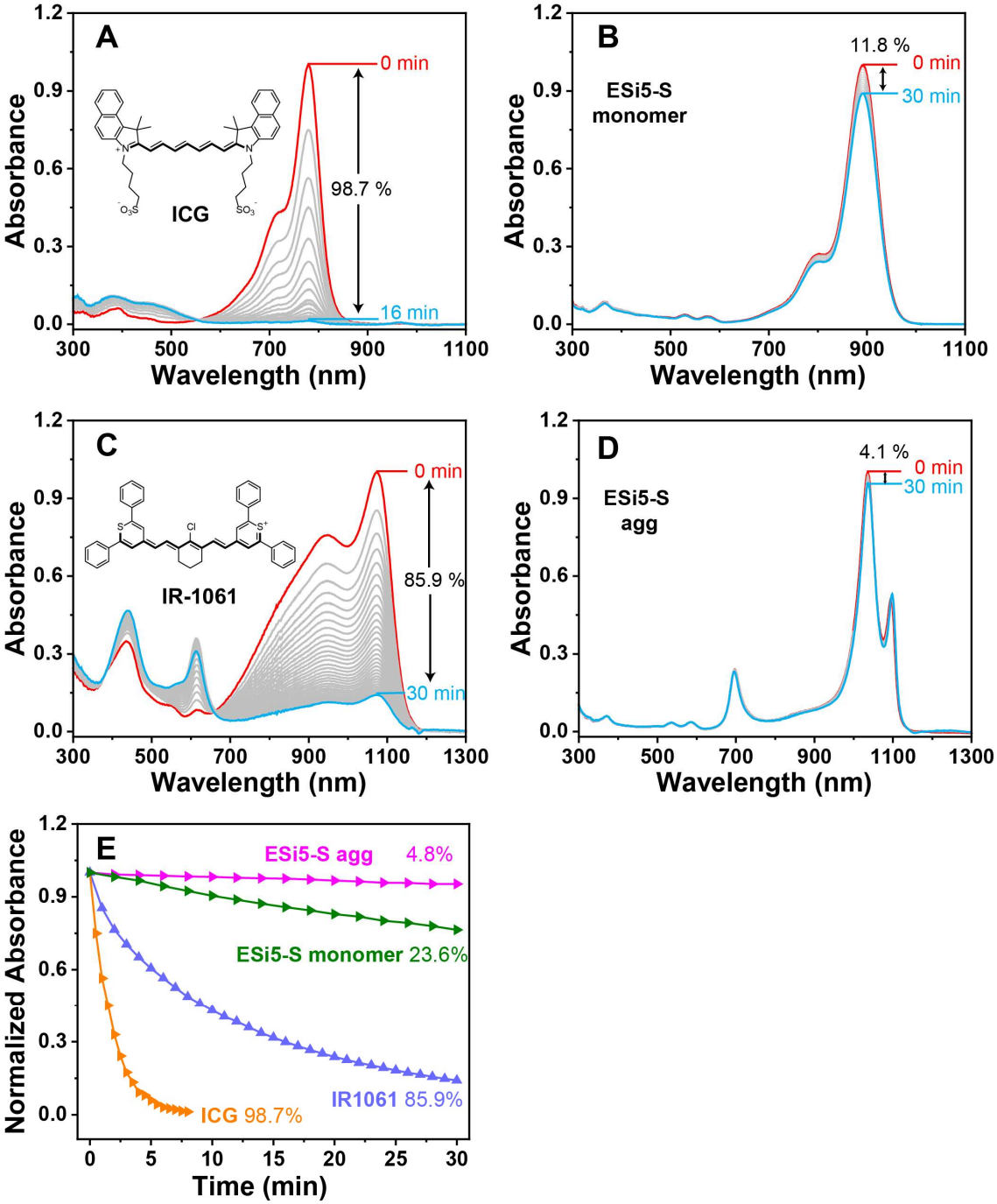

Supplementary Fig. 32: (A-D) Photo-stability tests of **ICG** in DMSO (Abs_{808}=0.2, 808 nm, 500 mW•cm^{-2}), **ESi5-S** monomer in DMSO (Abs_{808}=0.2, 808 nm, 500 mW•cm^{-2}), **IR-1061** in DMSO (Abs_{1064}=0.2, 1064 nm, 500 mW•cm^{-2}) and **ESi5-S agg** (Abs_{1064}=0.2, 1064 nm, 500 mW•cm^{-2}). (E) Absorbance decay at the absorption maximum with respect to irradiation duration.

Supplementary Table 3: The photobleaching rates and the bleaching half-life ($\tau_{1/2}$) of **ICG**, **ESi5-S** monomer, **IR-1061** and **ESi5-S agg**. The bleaching half-life ($\tau_{1/2}$) were calculated via fitting to an exponential decay Equation: $y = A_1 \times e^{(-x/\tau_{1/2})} + y_0$

	Photobleaching Rates	$\tau_{1/2}$	R^2
ICG	98.7%	3.560	0.999
ESi5-S monomer	11.8%	46.143	0.999
IR-1061	85.9%	10.297	0.995
ESi5-S agg	4.1%	~2636	0.998

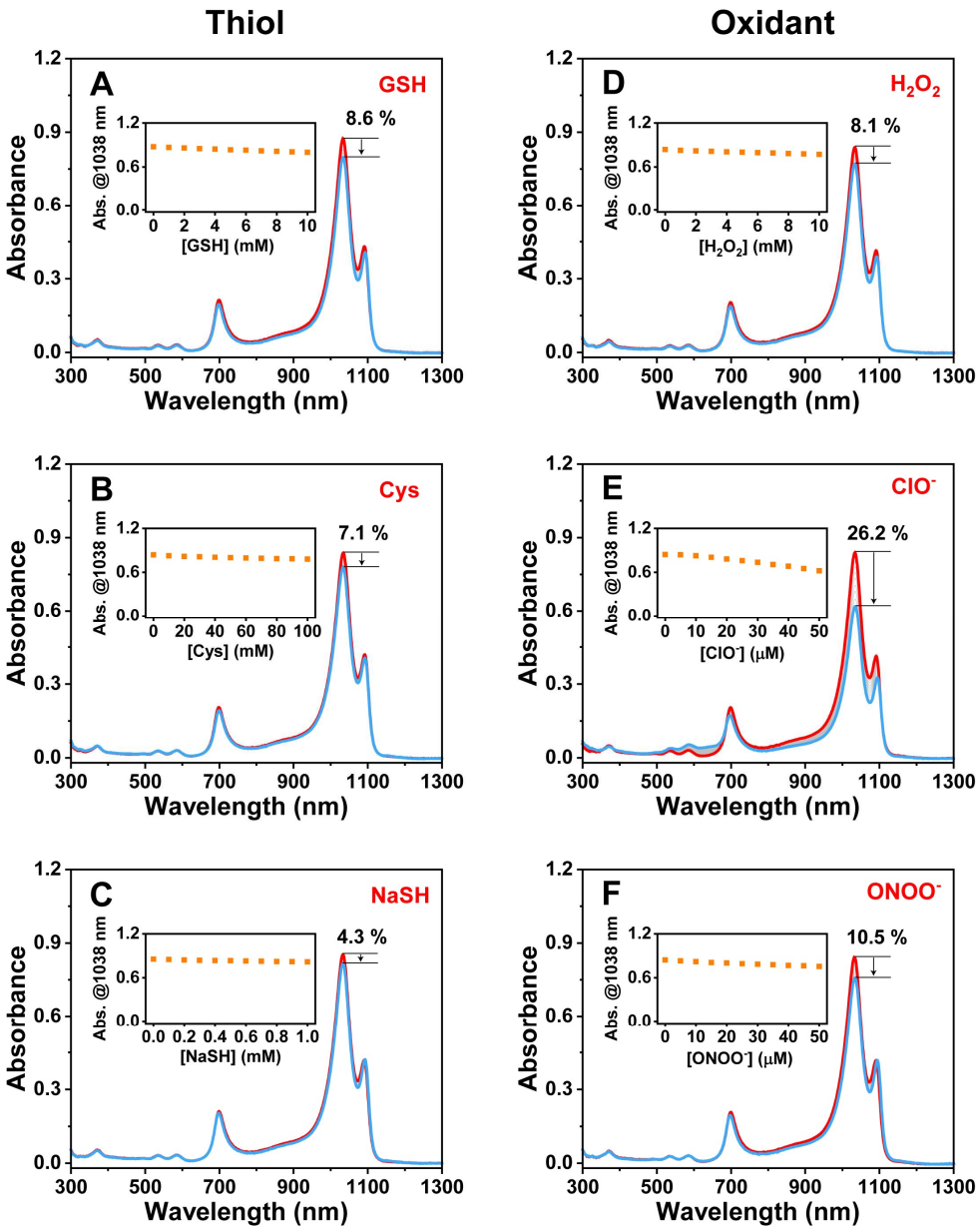

Supplementary Fig. 33: The chemo-stability of **ESi5-S agg** against (A) GSH, (B) Cys, (C) NaHS, (D) H_2O_2, (E) ClO^-, and (F) $ONOO^-$ in PBS buffer (pH = 7.4, 10 mM).

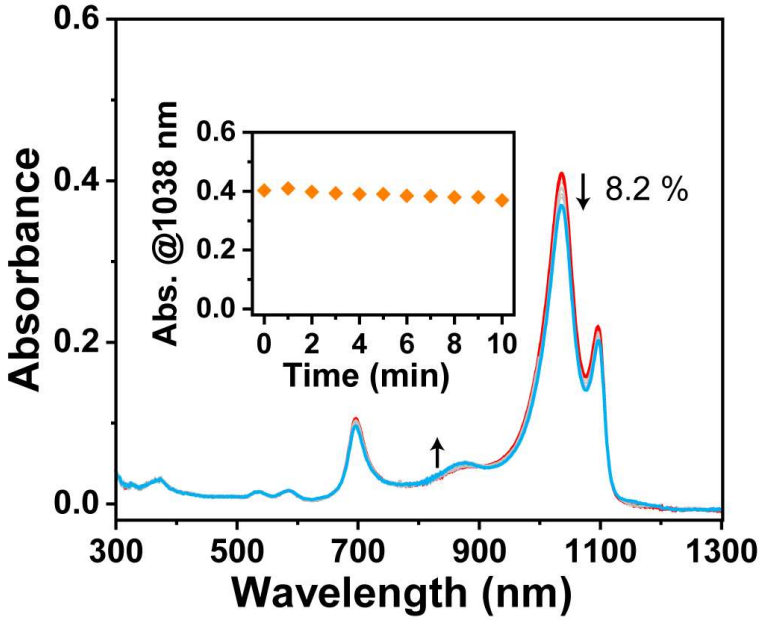

Supplementary Fig. 34: The absorption spectra of **ESi5-S agg** (5 μM) in PBS (pH = 7.4, 10 mM) sonicated for 1-10 min.

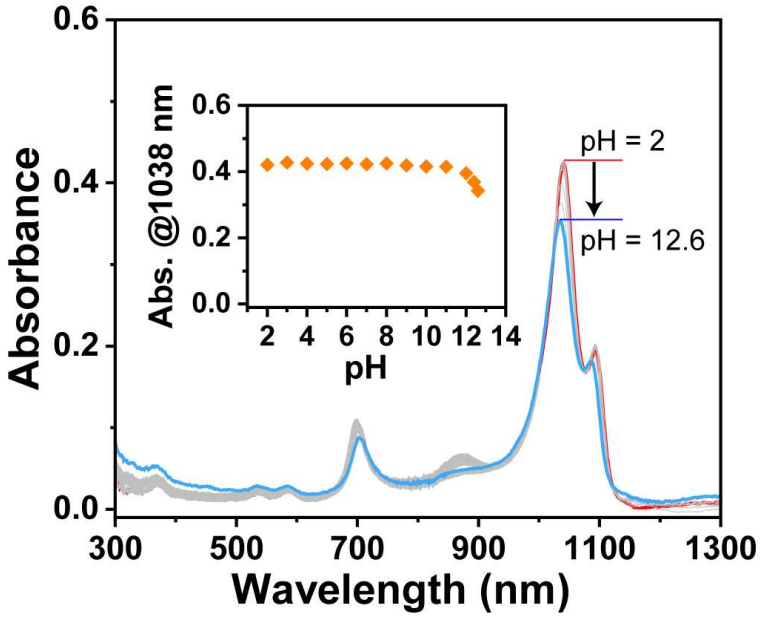

Supplementary Fig. 35: The pH stability of **ESi5-S agg** (5 μM).

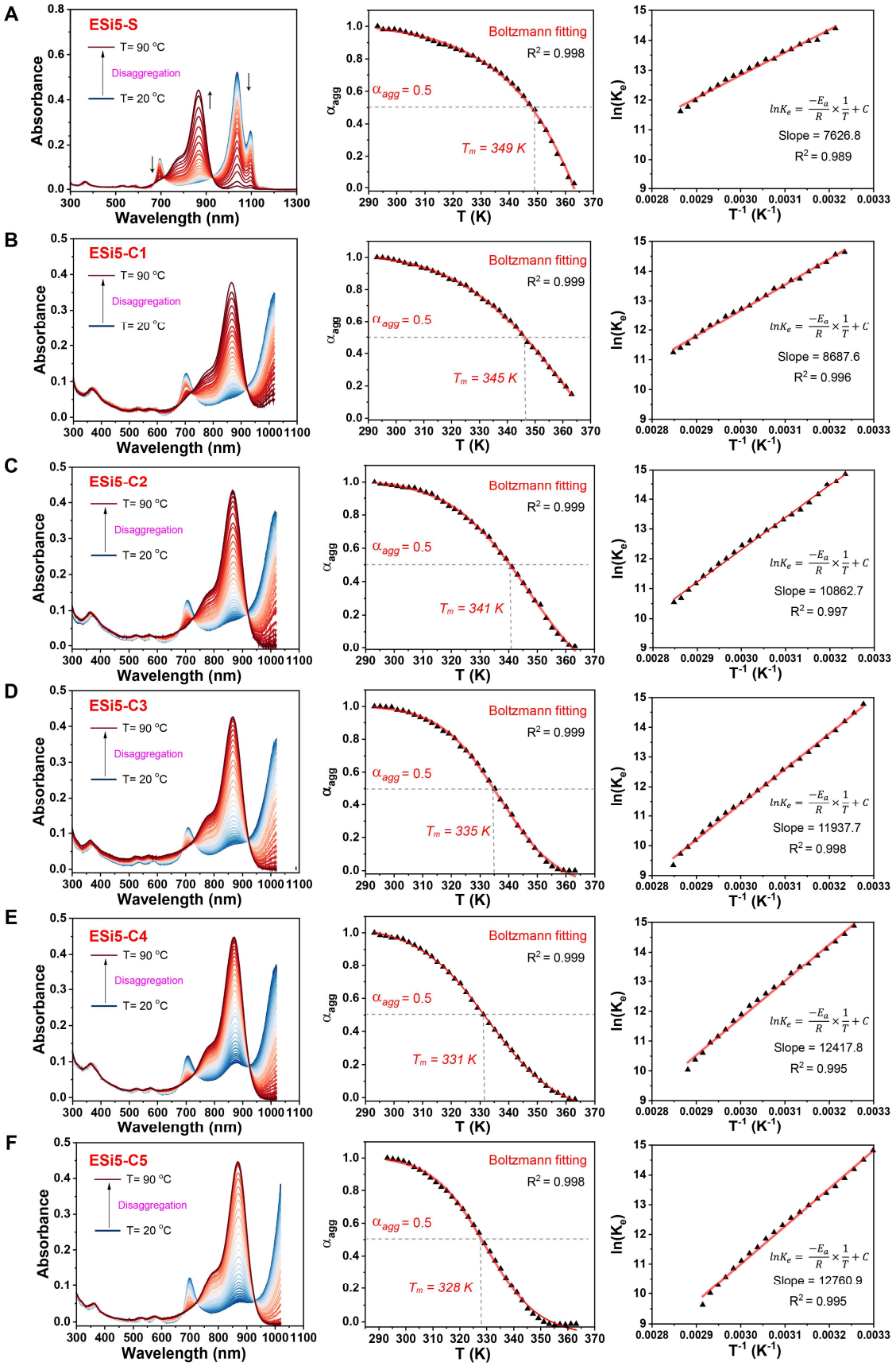

Supplementary Fig. 36: Temperature-dependent stability of (A) **ESi5-S agg** (5 μM), (B) **ESi5-C1 agg** (5 μM), (C) **ESi5-C2 agg** (5 μM), (D) **ESi5-C3 agg** (5 μM), (E) **ESi5-C4 agg** (5 μM), and (F) **ESi5-C5 agg** (5 μM), in PBS (pH = 7.4, 10 mM) with 5% methanol. Left: temperature-

dependent absorption spectra between 293 K and 363 K; middle: Boltzmann fit (y = A_2+ (A_1-A_2) / (1+exp (x-x_0)/dx)) of the fraction of aggregate (α_{agg}) as function of temperature; right: $ln(K_e)$ as function of 1/T. The Slope is equal to $-E_a/R$, where E_a is the activation energy and R is the gas constant.

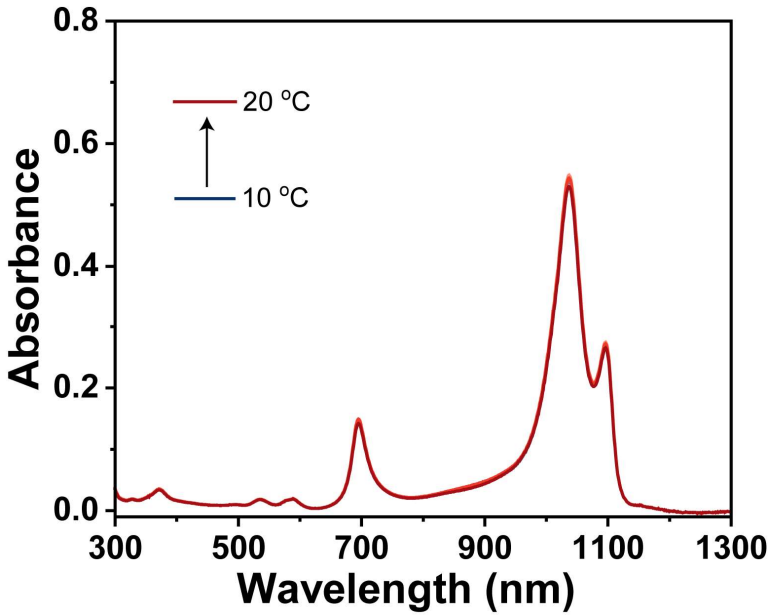

Supplementary Fig. 37: The UV-Vis absorption spectra of a solution of **ESi5-S agg** (5 μM in PBS, containing 5% methanol) at different temperature (10 °C to 20 °C).

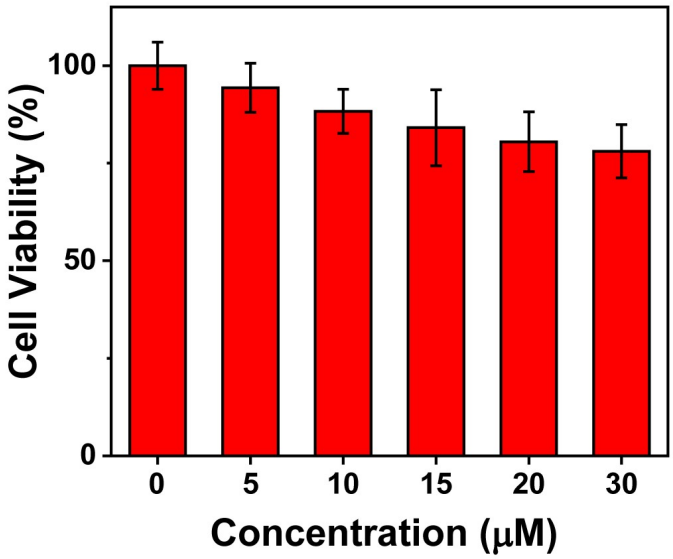

Supplementary Fig. 38: Viability of HeLa cells upon incubation with different concentration of **ESi5-S agg** (0-30 μM) for 24 hrs. (n=6, Data are presented as mean values +/- SD)

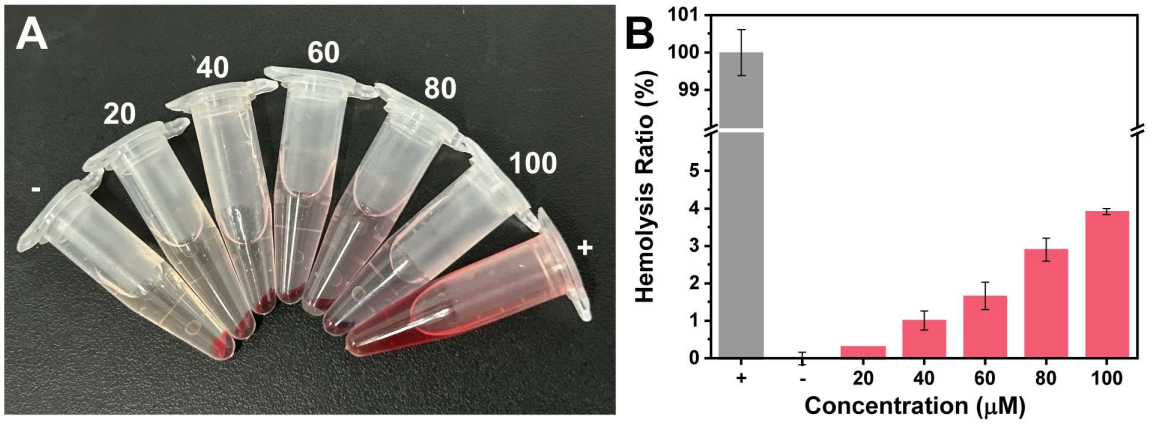

Supplementary Fig. 39: The hemolysis test of **ESi5-S agg**. A suspension of 2% sheep red blood cells was mixed with **ESi5-S agg** (0-100 μM), compared to Triton X-100 (+, 2%). (n = 3, Data are presented as mean values +/- SD)

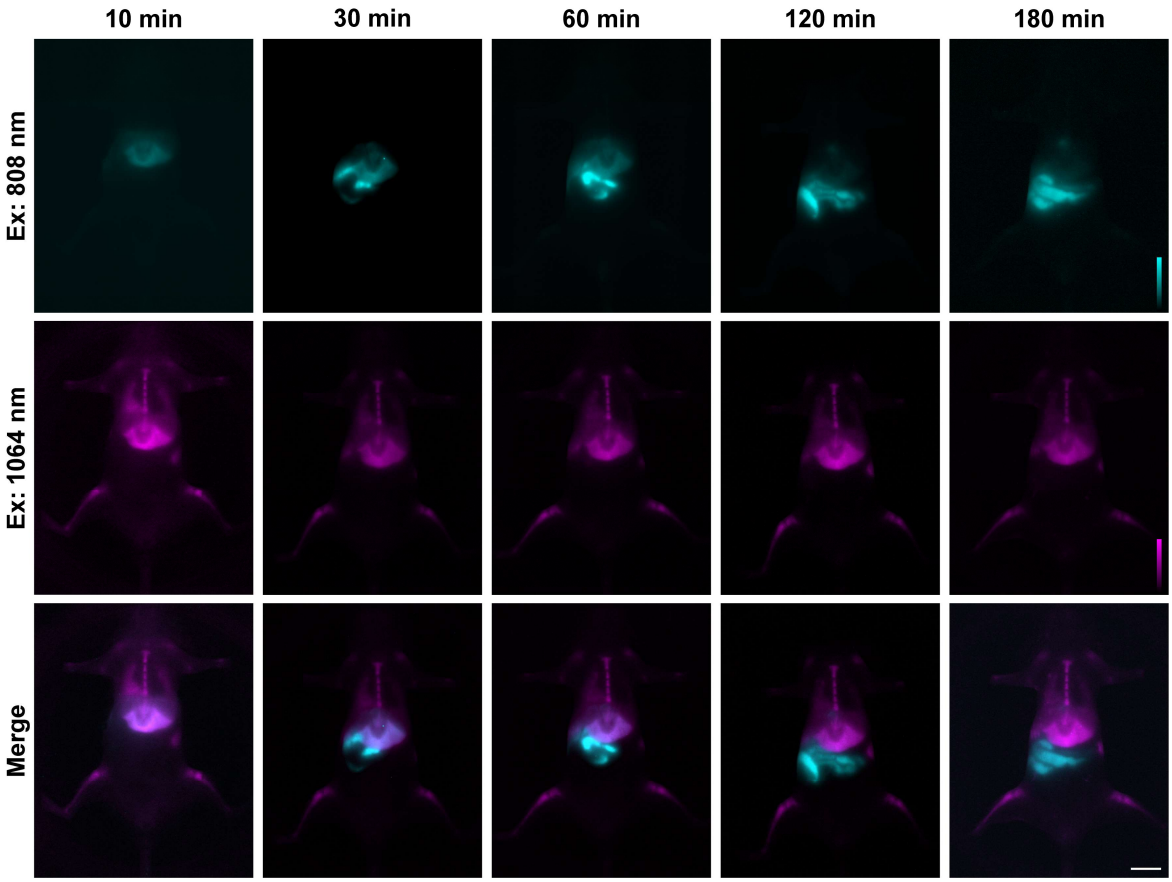

Supplementary Fig. 40: The dual-channel fluorescence images of BALB/c mice in supine position acquired 0 min, 30 min, 60 min, 120 min, or 180min post *i.v.* injection of **ESi5-S agg**. Scale bar: 10 mm. 808 nm channel: λ_{ex} = 808 nm (60 mW•cm^{-2}), long pass filter: 1200 nm, exposure time: 100 ms. 1064 nm channel: λ_{ex} = 1064 nm (80 mW•cm^{-2}), long pass filter: 1200+1350 nm, exposure time: 500 ms.

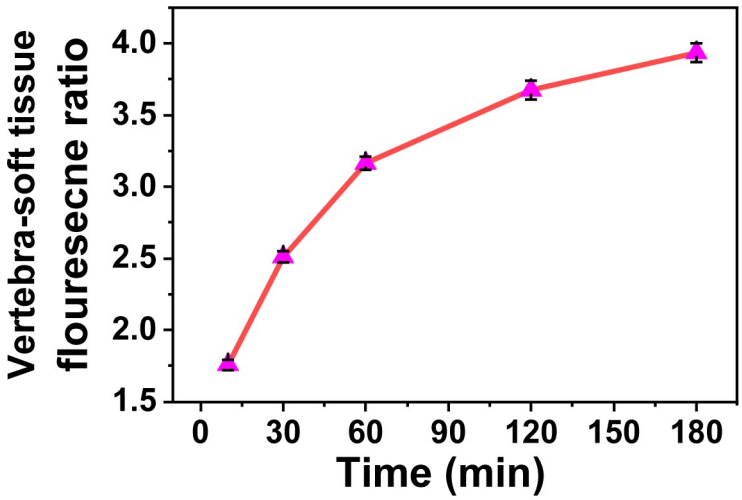

Supplementary Fig. 41: The vertebra-soft tissue fluorescence ratio of mouse post-injection of **ESi5-S agg** (500 μM in PBS, 100 μL). (n=3, Data are presented as mean values +/- SD)

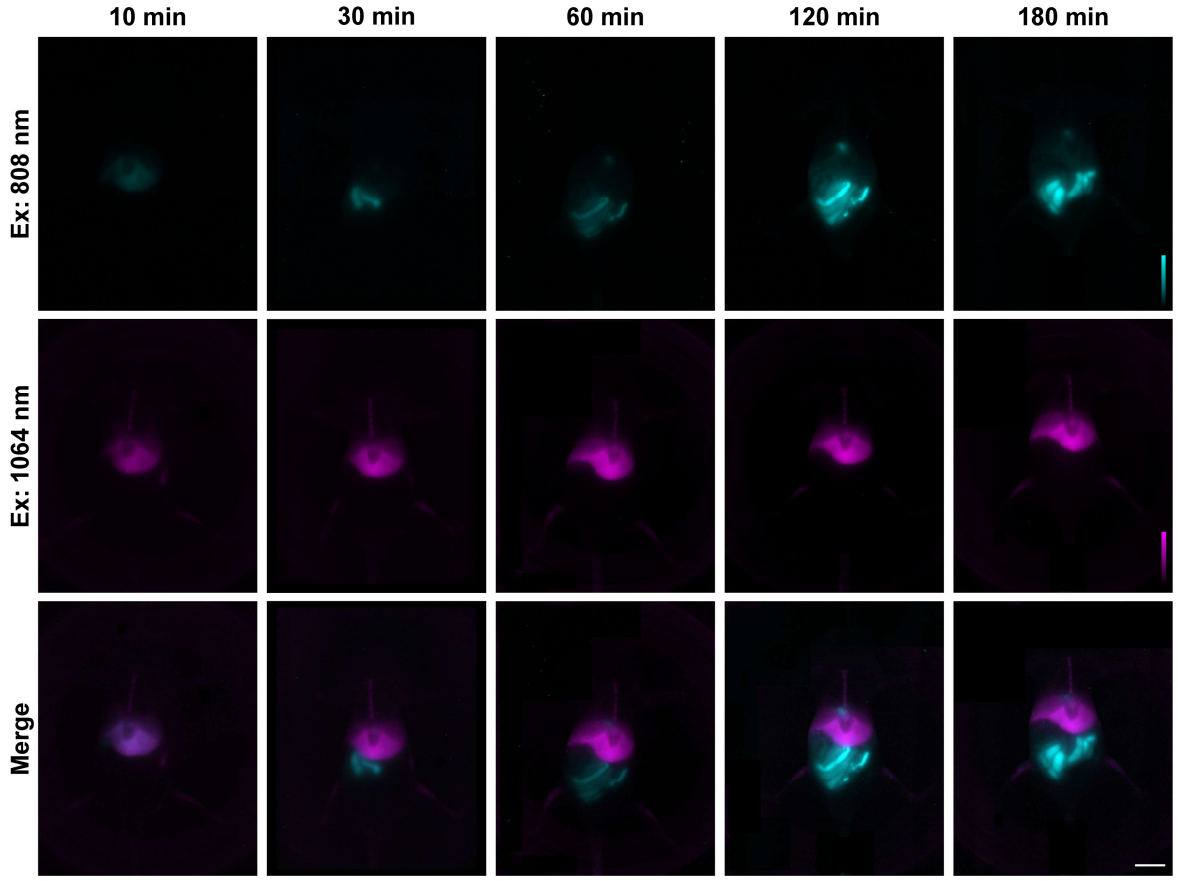

Supplementary Fig. 42: The repeat dual-channel fluorescence images of BALB/c mice in supine position acquired 0 min, 30 min, 60 min, 120 min, or 180min post *i.v.* injection of **ESi5-S agg**. Scale bar: 10 mm. 808 nm channel: λ_{ex} = 808 nm (60 mW•cm^{-2}), long pass filter: 1200 nm, exposure time: 100 ms. 1064 nm channel: λ_{ex} = 1064 nm (80 mW•cm^{-2}), long pass filter: 1200+1350 nm, exposure time: 500 ms.

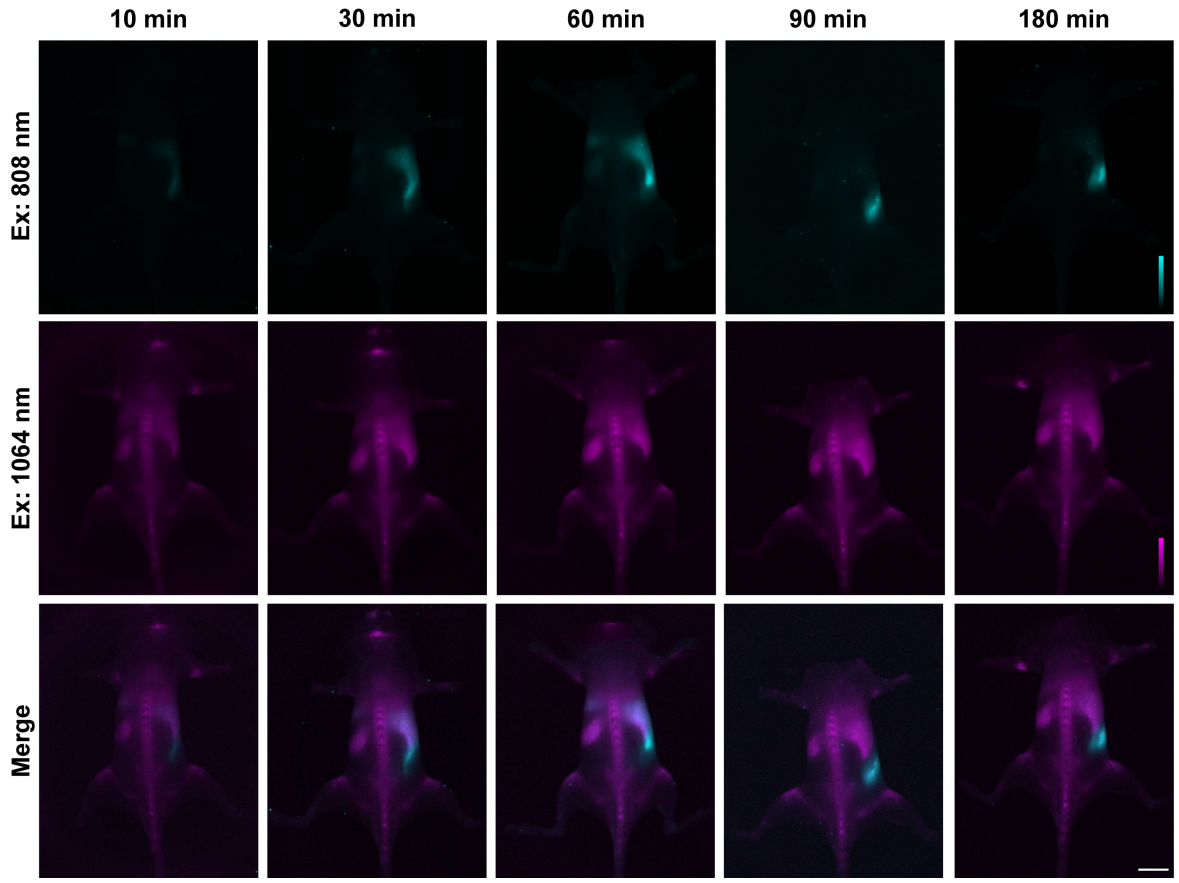

Supplementary Fig. 43: The dual-channel fluorescence images of BALB/c mice in prone position acquired 0 min, 30 min, 60 min, 120 min, or 180min post *i.v.* injection of **ESi5-S agg**. Scale bar: 10 mm. 808 nm channel: λ_{ex} = 808 nm (60 mW•cm^{-2}), long pass filter: 1200 nm, exposure time: 100 ms. 1064 nm channel: λ_{ex} = 1064 nm (80 mW•cm^{-2}), long pass filter: 1200+1350 nm, exposure time: 500 ms.

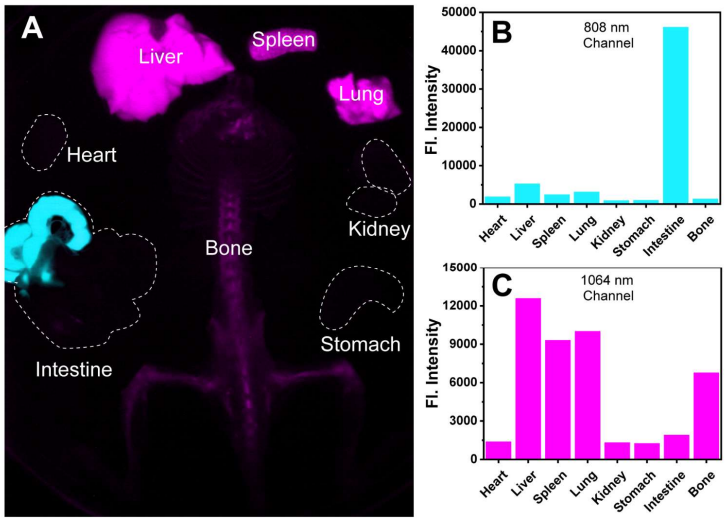

Supplementary Fig. 44: (A). The fluorescence image of the tissue distribution in mice after injection of **ESi5-S agg**. The major tissues including the heart, liver, spleen, lung, kidney, stomach, intestine, and bone. (B, C). The fluorescence intensity of major tissues in 808 nm channel (B) and 1064 nm channel (C) 180 min post-injection of **ESi5-S agg**.

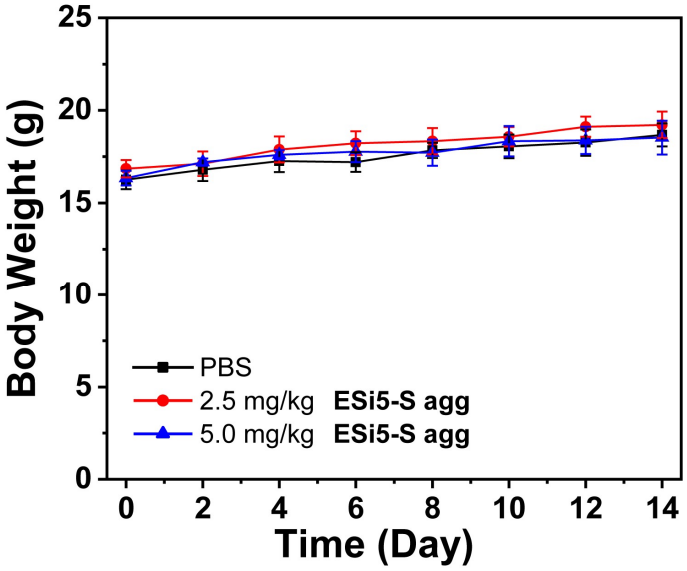

Supplementary Fig. 45: The change of the body weight of BALB/c mice after intravenous injected with PBS (100 μL), 2.5 mg/kg **ESi5-S agg** and 5.0mg/kg **ESi5-S agg**. (n=6, Data are presented as mean values +/- SD)

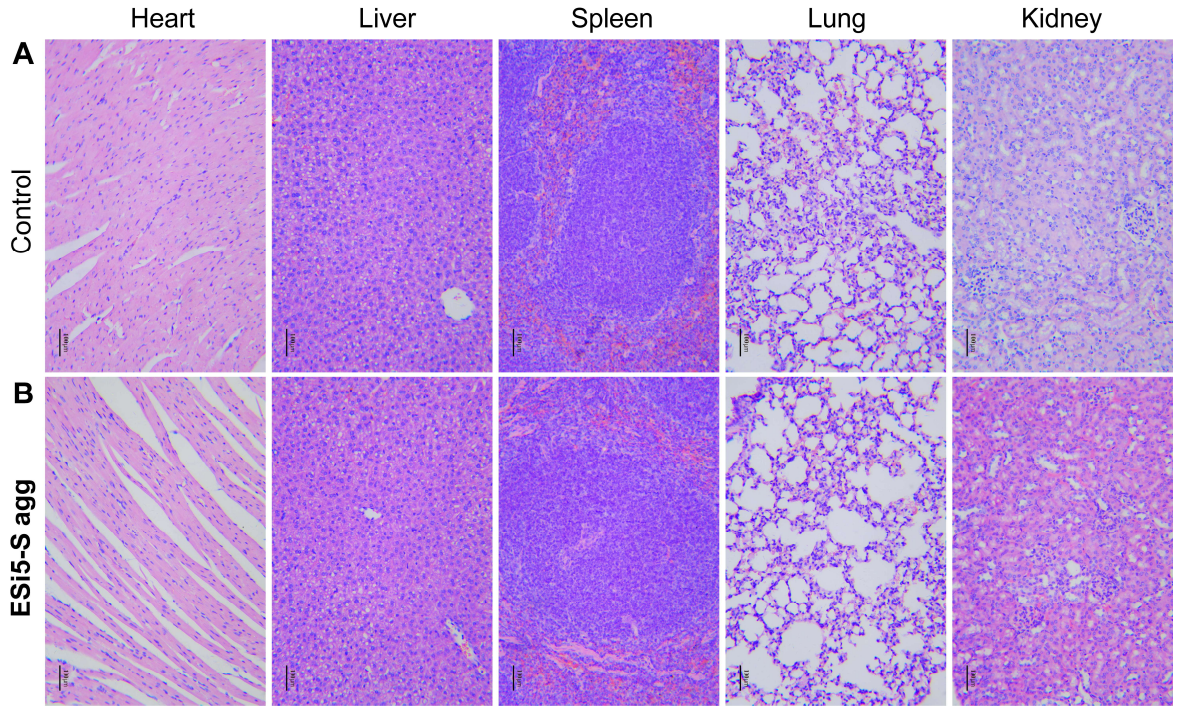

Supplementary Fig. 46: H&E images of major organs (including heart, liver, spleen, lung and kidney) collected from (A) BALB/c mice treated with PBS (100 μL) and (B) BALB/c mice at 24 h post-injection of **ESi5-S agg** (2.5 mg/kg). No obvious organ damage or lesion was observed for **ESi5-S agg** injected mice. Scale bar: 100 μm.

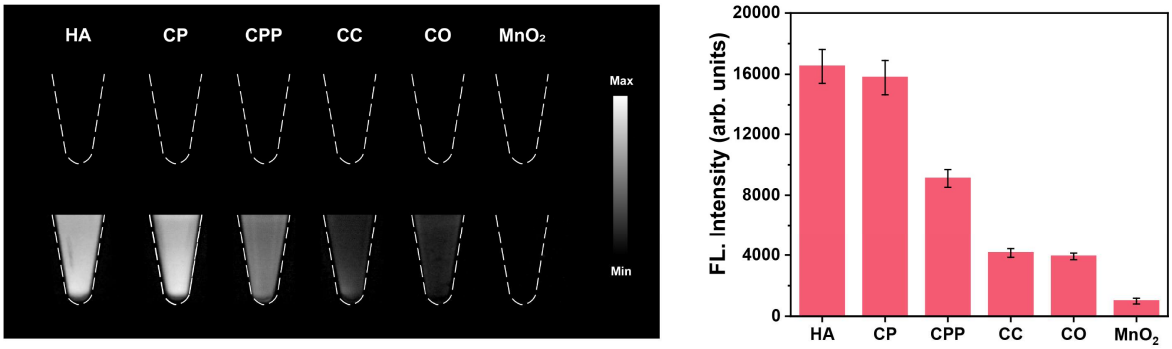

Supplementary Fig. 47: The fluorescence image (A) and fluorescence intensity (B) of **ESi5-S agg** binding with different calcium-containing salts and MnO_2. Note: hydroxyapatite (HA), calcium phosphate (CP), calcium pyrophosphate salts (CPP), calcium carbonate (CC), calcium oxalate (CO), and manganese dioxide (MnO_2).

Synthesis and characterization

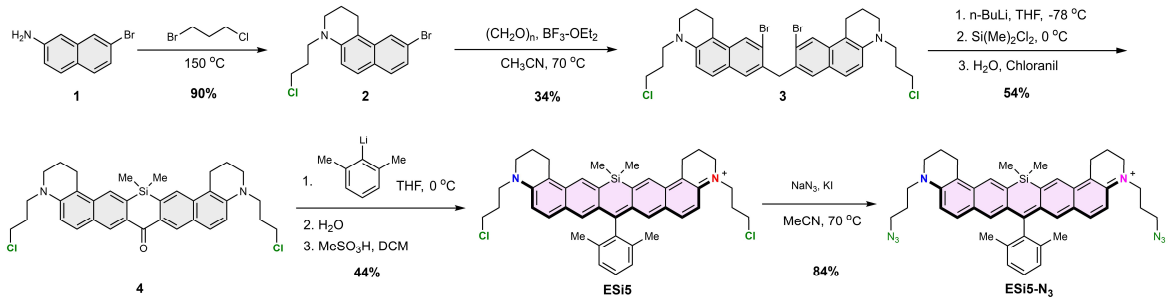

Supplementary Fig. 48: The synthetic scheme of **ESi5-N_3**

Synthesis of **2.** 7-bromo-2-naphthylamine (20.0 g, 90.06 mmol, 1 equiv.) was dissolved in 1-bromo-3-chloropropane (44.6 mL, 450.28 mmol, 5 equiv.) in a 250 mL round-bottomed flask. The reaction was stirred at 150 °C for 24 h before quenched by additional of H_2O (100 mL). The mixture was cooled down to room temperature, and extracted with CH_2Cl_2 (3 × 50 mL). The organic layer was dried over anhydrous Na_2SO_4, filtered and evaporated to dryness. The residue was purified by chromatography column (silica, PE/EA, 50:1, v/v) to give **2** (27.6 g, 90% yield) as a colorless oil. The ^{1}H-NMR of the compound **2** was verified to be identical with literature spectra.[29]

Synthesis of **3.** Compound **2** (2.0 g, 5.91 mmol, 1 equiv), and BF_3•OEt_2 (0.2 mL) and paraformaldehyde (0.35 g, 11.8 mmol, 2 equiv) was dissolved in MeCN (20 mL) in a 100 mL pressure bottle and the mixture was stirred at 80 °C for 6 hours. The reaction mixture was cooled to room temperature and quenched by H_2O (50 mL). The reaction mixture was extracted with EtOAc (3 × 20 mL), dried over anhydrous Na_2SO_4, filter and evaporated. The residue was purified by chromatography column (silica, PE/EA, 50:1→20:1, v/v) to give **3** (0.69 g, 34% yield) as a yellow solid. The ^{1}H-NMR of the compound **3** was verified to be identical with literature spectra.[29]

Synthesis of **4.** A solution compound **3** (1.0 g, 1.45 mmol, 1 equiv.) in anhydrous THF (20 mL) was cooled down to -78 °C under argon atmosphere. n-BuLi (2.5 M, 1.28 mL, 3.19 mmol, 5 equiv.) was added into the mixture and stirred for 30 minutes. Upon warmed to

room temperature, a solution of Me_2SiCl_2 (2.5 M, 1.28 mL, 3.19 mmol, 2.2 equiv.) was added, and the mixture was stirred for an additional 1 hours. The reaction mixture was then quenched with the addition of saturated NH_4Cl, extracted with EtOAc (3 × 20 mL), dried over anhydrous Na_2SO_4, filter and evaporated. The residue was dissolved in EtOAc (20 mL) and tetrachlorobenzoquinone (1 g) was added, then the mixture was stirred overnight. The reaction mixture was then quenched with the addition of H_2O, extracted with EtOAc (3 × 20 mL), dried over anhydrous Na_2SO_4, filter and evaporated. The residue was purified by chromatography column (silica, PE/EA, 20:1→5:1, v/v) to give **4** (0.48 g, 54% yield) as a yellow solid. The ^{1}H-NMR of the compound **4** was verified to be identical with literature spectra.[29]

Synthesis of **ESi5.** A solution of 1-bromo-2,6-dimethylbenzene (0.56 mL, 3.99 mmol, 6 equiv.) in anhydrous THF (10 mL) was cooled down to -78 °C under argon atmosphere. n-BuLi (2.5 M, 1.33 mL, 3.32 mmol, 5 equiv.) was added, and the mixture was stirred at -78 °C for 20 minutes. Then the mixture was added to a solution of compound **4** (0.4 g, 0.66 mmol, 1 equiv.) in anhydrous THF (10 mL) at 0 °C. The reaction mixture was warmed to room temperature for 20 minutes and then quenched by MeOH (5 mL). $MeSO_3H$ (0.5 mL) was added to the mixture, and then extracted with CH_2Cl_2 (3 × 20 mL), dried with anhydrous Na_2SO_4, filter and evaporated. The residue was purified by chromatography column (silica, DCM/MeOH, 100:1→20:1, v/v) to give **ESi5** (201 mg, 44% yield) as a deep violet solid. The ^{1}H-NMR of the compound **ESi5** was verified to be identical with literature spectra.[29]

Synthesis of **ESi5-N_3. ESi5** (50 mg, 0.07 mmol, 1 equiv.), sodium azide (14 mg, 0.21 mmol, 3 equiv.) and KI (10 mg) were dissolved in MeCN (10 mL) and stirred at 70 °C for 8 h. Upon cooling to room temperature, the mixture was extracted with EtOAc (3 × 20 mL) and dried with anhydrous Na_2SO_4, filter and evaporated. The residue was purified by chromatography column (silica, DCM/MeOH, 100:1→20:1, v/v) to give **ESi5-N_3** (43 mg, 84% yield) as a deep violet solid. The ^{1}H-NMR of the compound **ESi5-N_3** was verified to be identical with literature spectra.[29]

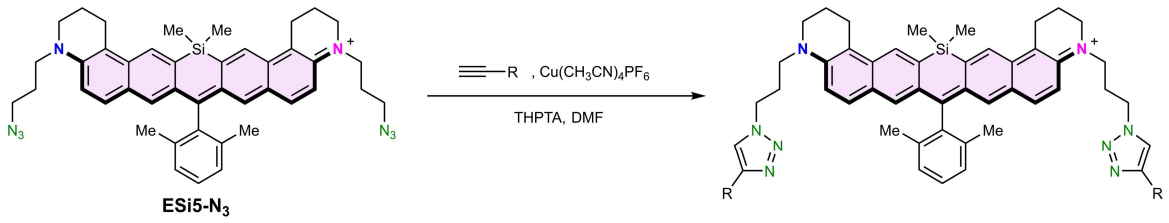

Supplementary Fig. 49: The general synthetic scheme of water-soluble modified ESi5.

General Method for Click Reaction: To a solution of **ESi5-N_3** (0.072 mmol, 50.0 mg) and the corresponding terminal alkyne-containing compound (0.284 mmol, 4.0 eq.) dissolved in DMF (20 mL) was added a solution of $[(CH_3CN)_4Cu]PF_6$ (0.028 mmol, 9.5 mg, 0.4 eq.) and tris(3-hydroxypropyltriazolylmethyl) amine (THPTA, 0.014 mmol, 6.5 mg, 0.2 eq.) in water (1 mL) with stirring. The reaction ran at room temperature for 2 h. The mixture was evaporated to dryness and the crude product was purified with a chromatograph column over reverse phase silica using H_2O/MeOH (v/v = 1/1) as the eluent. The fractions containing the product were lyophilized to give corresponding compound as a dark red

powder.

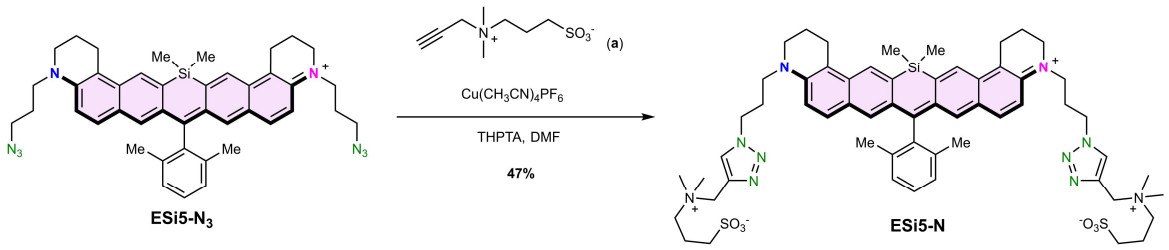

Supplementary Fig. 50: The synthetic scheme of **ESi5-NS**.

Synthesis of **ESi5-NS**: Compound **ESi5-NS** was prepared following the general method with **a** (purchased from Leyan) in an isolated yield of 47% (37.5 mg). ^{1}H NMR (600 MHz, CD_3OD) δ 8.48 (s, 2H), 8.10 (s, 2H), 7.54 (s, 2H), 7.47 (t, J = 7.7 Hz, 1H), 7.41 (d, J = 9.4 Hz, 2H), 7.33 (d, J = 7.7 Hz, 2H), 7.17 (d, J = 9.4 Hz, 2H), 4.67 (s, 4H), 4.59 (t, J = 7.0 Hz, 4H), 3.74 (t, J = 7.5 Hz, 4H), 3.67 (t, J = 5.5 Hz, 4H), 3.48 – 3.39 (m, 4H), 3.15 (t, J = 6.0 Hz, 4H), 3.13 (s, 12H), 2.86 (t, J = 6.4 Hz, 4H), 2.46 – 2.36 (m, 4H), 2.34 – 2.23 (m, 4H), 2.20 – 2.10 (m, 4H), 2.01 (s, 6H), 0.65 (s, 6H). ^{13}C NMR (151 MHz, CD_3OD) δ 165.35, 153.55, 143.77, 139.19, 137.93, 136.85, 136.54, 133.97, 132.56, 130.63, 130.26, 129.33, 117.99, 63.33, 59.16, 51.93, 51.14, 50.00, 48.83, 29.15, 24.33, 22.49, 20.32, 0.39. HRMS (ESI) (m/z): $[M]^+$ calculated. for $C_{59}H_{77}N_{10}O_6S_2Si^+$, 1113.5233; found: 1113.5233.

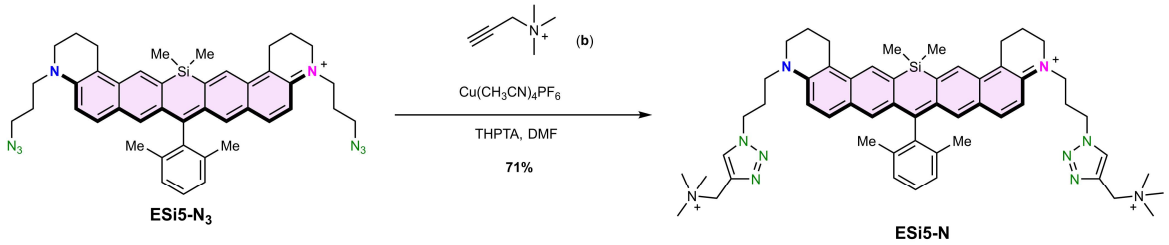

Supplementary Fig. 51: The synthetic scheme of **ESi5-N**.

Synthesis of **ESi5-N**: Compound **ESi5-N** was prepared following the general method with with **b** (purchased from Leyan) in an isolated yield of 71% (45.2 mg). ^{1}H NMR (600 MHz, CD_3OD) δ 8.45 (s, 2H), 8.11 (s, 2H), 7.55 (s, 2H), 7.47 (t, J = 7.7 Hz, 1H), 7.42 (d, J = 8.6 Hz, 2H), 7.33 (d, J = 7.6 Hz, 2H), 7.18 (d, J = 9.4 Hz, 2H), 4.70 (s, 4H), 4.62 (t, J = 7.0 Hz, 4H), 3.76 (t, J = 7.4 Hz, 4H), 3.67 (s, 4H), 3.16 (s, 22H), 2.45 – 2.35 (m, 4H), 2.18 – 2.10 (m, 4H), 2.02 (s, 6H), 0.66 (s, 6H). ^{13}C NMR (151 MHz, CD_3OD) δ 153.53, 143.82, 137.31, 136.76, 136.52, 135.31, 133.99, 132.57, 130.61, 130.01, 129.30, 117.99, 61.56, 53.86, 51.84, 51.13, 33.16, 29.19, 24.33, 22.48, 20.33, 0.37. HRMS (ESI) (m/z): $[M]^+$ calculated. for $C_{55}H_{71}N_{10}Si^{3+}$, 899.5616; m/z= 299.8539; found: 299.8606.

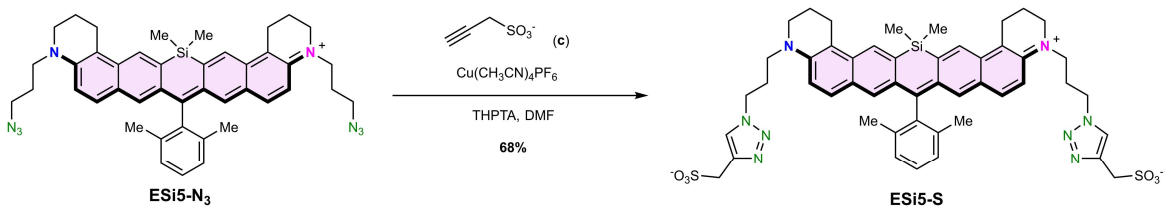

Supplementary Fig. 52: The synthetic scheme of **ESi5-S**.

Synthesis of **ESi5-S**: Compound **ESi5-S** was prepared following the general method with

with **c** (purchased from Leyan) in an isolated yield of 68% (48.1 mg). ^{1}H NMR (600 MHz, CD_3OD) δ 8.08 (s, 2H), 8.00 (s, 2H), 7.54 (s, 2H), 7.46 (t, *J* = 7.7 Hz, 1H), 7.42 (d, *J* = 9.4 Hz, 2H), 7.32 (d, *J* = 7.7 Hz, 2H), 7.06 (d, *J* = 9.4 Hz, 2H), 4.52 (t, *J* = 6.5 Hz, 4H), 3.66 (t, *J* = 7.5 Hz, 4H), 3.61 (t, *J* = 5.2 Hz, 4H), 3.12 (t, *J* = 6.3 Hz, 4H), 2.44 – 2.26 (m, 4H), 2.18 – 2.07 (m, 4H), 2.01 (s, 7H), 0.64 (s, 6H). ^{13}C NMR (151 MHz, CD_3OD) δ 171.09, 153.44, 143.78, 142.25, 139.10, 137.90, 136.66, 133.91, 132.48, 131.27, 130.59, 129.29, 126.04, 117.89, 117.84, 51.69, 50.99, 49.98, 29.06, 24.31, 22.46, 20.33. ESI-HRMS (m/z): $[M]^+$ calculated for $C_{49}H_{53}N_8Na_2O_6S_2Si^+$, 987.3089; found: 987.3097.

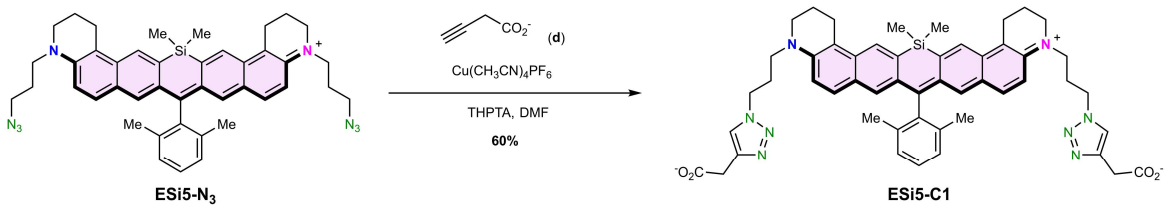

Supplementary Fig. 53: The synthetic scheme of **ESi5-C1**.

Synthesis of **ESi5-C1**: Compound **ESi5-C1** was prepared following the general method with with **d** (purchased from Leyan) in an isolated yield of 60% (47.4 mg). ^{1}H NMR (600 MHz, CD_3OD) δ 8.08 (s, 2H), 7.86 (s, 2H), 7.52 (s, 2H), 7.45 (t, *J* = 7.7 Hz, 1H), 7.39 (d, *J* = 9.4 Hz, 2H), 7.31 (d, *J* = 7.8 Hz, 2H), 7.08 (d, *J* = 9.4 Hz, 2H), 4.50 (t, *J* = 6.7 Hz, 4H), 3.68 (t, *J* = 7.5 Hz, 4H), 3.61 (t, *J* = 5.4 Hz, 4H), 3.12 (t, *J* = 6.3 Hz, 4H), 2.36 – 2.28 (m, 4H), 2.15 – 2.07 (m, 4H), 1.99 (s, 6H), 0.64 (s, 6H). ^{13}C NMR (151 MHz, CD_3OD) δ 178.27, 170.96, 153.42, 143.70, 140.21, 139.15, 137.88, 136.68, 136.48, 133.92, 132.53, 130.59, 129.28, 125.17, 117.93, 117.87, 51.73, 51.08, 49.98, 29.13, 24.29, 22.45, 20.32, 0.36. ESI-HRMS (m/z): $[M]^+$ calculated. for $C_{51}H_{55}N_8O_4Si^+$, 871.4110; found: 871.4113.

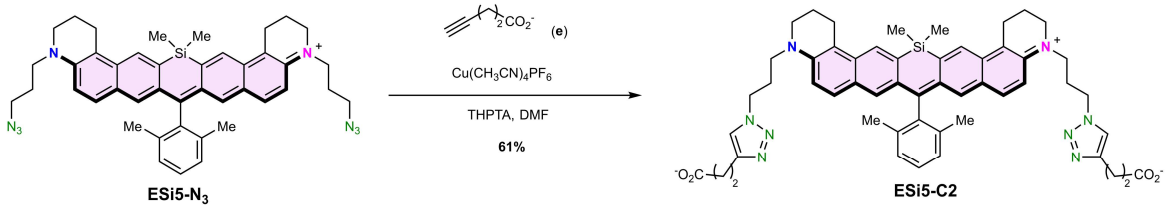

Supplementary Fig. 54: The synthetic scheme of **ESi5-C2**.

Synthesis of **ESi5-C2**: Compound **ESi5-C2** was prepared following the general method with with **e** (purchased from Leyan) in an isolated yield of 61% (37.1 mg).^{1}H NMR (600 MHz, CD_3OD) δ 8.08 (s, 2H), 7.74 (s, 2H), 7.54 (s, 2H), 7.47 (t, J = 7.7 Hz, 1H), 7.39 (d, J = 9.4 Hz, 2H), 7.33 (d, J = 7.8 Hz, 2H), 7.06 (d, J = 9.4 Hz, 2H), 4.47 (t, J = 6.6 Hz, 4H), 3.67 (t, *J* = 7.4 Hz, 4H), 3.59 (t, *J* = 5.5 Hz, 4H), 3.11 (t, J = 6.4 Hz, 4H), 2.93 (t, J = 7.3 Hz, 4H), 2.54 (t, J = 7.3 Hz, 4H), 2.36 – 2.26 (m, 4H), 2.17 – 2.07 (m, 4H), 2.01 (s, 6H), 0.64 (s, 6H).^{13}C NMR (151 MHz, CD_3OD) δ 168.70, 165.65, 149.70, 143.80, 137.92, 136.70, 136.50, 132.51, 131.28, 130.61, 129.30, 123.95, 117.90, 117.83, 51.73, 51.15, 49.99, 38.44, 29.05, 24.28, 23.68, 22.43, 20.35.HRMS (ESI) (m/z): $[M]^+$ calculated. for $C_{53}H_{59}N_8O_4Si^+$, 899.4424; found: 899.4427.

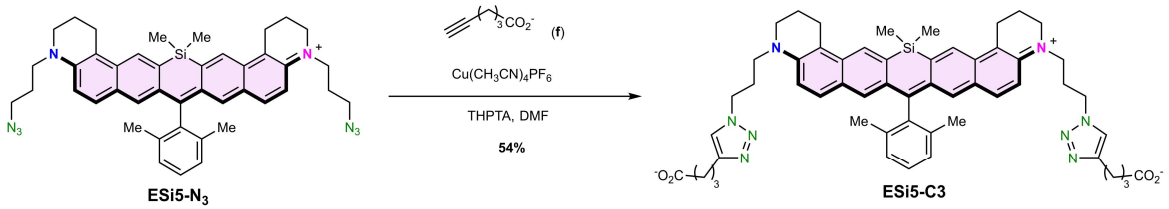

Supplementary Fig. 55: The synthetic scheme of **ESi5-C3**.

Synthesis of **ESi5-C3**: Compound **ESi5-C3** was prepared following the general method with with **f** (purchased from Leyan) in an isolated yield of 54% (35.6 mg). ^{1}H NMR (600 MHz, CD_3OD) δ 8.08 (s, 2H), 7.76 (s, 2H), 7.54 (s, 2H), 7.46 (t, J = 7.7 Hz, 1H), 7.39 (d, J = 9.2 Hz, 2H), 7.32 (d, J = 7.7 Hz, 2H), 7.08 (d, J = 9.4 Hz, 2H), 4.48 (t, J = 6.7 Hz, 4H), 3.68 (d, J = 7.4 Hz, 4H), 3.60 (t, *J* = 5.5 Hz, 4H), 3.12 (t, J = 6.1 Hz, 4H), 2.68 (t, J = 7.5 Hz, 4H), 2.38 – 2.28 (m, 4H), 2.17 (t, J = 7.4 Hz, 4H), 2.14 – 2.06 (m, 4H), 2.01 (s, 6H), 1.96 – 1.84 (m, 4H), 0.64 (s, 6H). ^{13}C NMR (151 MHz, CD_3OD) δ 179.86, 174.57, 153.44, 149.65, 143.81, 139.16, 137.92, 136.71, 136.47, 133.93, 132.52, 130.61, 129.29, 123.98, 117.91, 117.82, 51.73, 51.17, 49.98, 38.50, 29.07, 27.67, 26.53, 24.27, 22.42, 20.33. HRMS (ESI) (m/z): $[M]^+$ calculated. for $C_{55}H_{63}N_8O_4Si^+$, 927.4737; found: 927.4744.

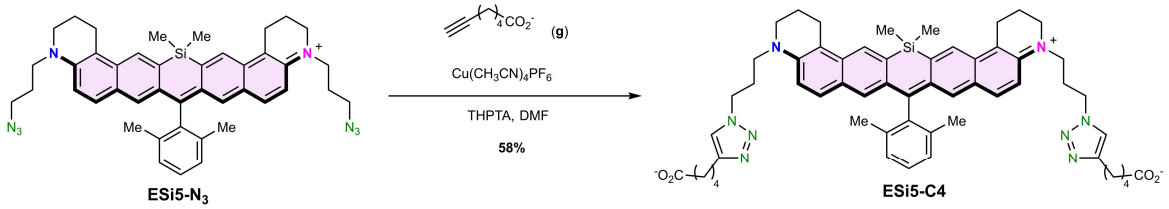

Supplementary Fig. 56: The synthetic scheme of **ESi5-C4**.

Synthesis of **ESi5-C4**: Compound **ESi5-C4** was prepared following the general method with with **g** (purchased from Leyan) in an isolated yield of 58% (39.2 mg). ^{1}H NMR (600 MHz, CD_3OD) δ 8.08 (s, 2H), 7.74 (s, 2H), 7.54 (s, 2H), 7.47 (t, J = 7.7 Hz, 1H), 7.38 (d, J = 9.4 Hz, 2H), 7.33 (d, J = 7.7 Hz, 2H), 7.07 (d, J = 9.5 Hz, 2H), 4.48 (t, J = 6.6 Hz, 4H), 3.69 (t, J = 7.4 Hz, 4H), 3.60 (t, J = 5.6 Hz, 4H), 3.11 (t, J = 6.4 Hz, 4H), 2.64 (t, J = 7.1 Hz, 4H), 2.41 – 2.30 (m, 4H), 2.24 – 2.15 (m, 4H), 2.13 – 2.04 (m, 4H), 2.01 (s, 6H), 1.72 – 1.51 (m, 8H), 0.65 (s, 6H). ^{13}C NMR (151 MHz, CD_3OD) δ 171.12, 169.56, 153.41, 149.64, 143.78, 139.16, 137.90, 136.68, 136.42, 133.92, 132.52, 131.26, 130.61, 129.29, 123.87, 117.92, 117.80, 51.70, 51.19, 49.97, 30.55, 29.02, 26.80, 26.42, 24.24, 22.38, 20.34, 0.36. HRMS (ESI) (m/z): $[M]^+$ calculated. for $C_{57}H_{67}N_8O_4Si^+$, 955.5050; found: 955.5056.

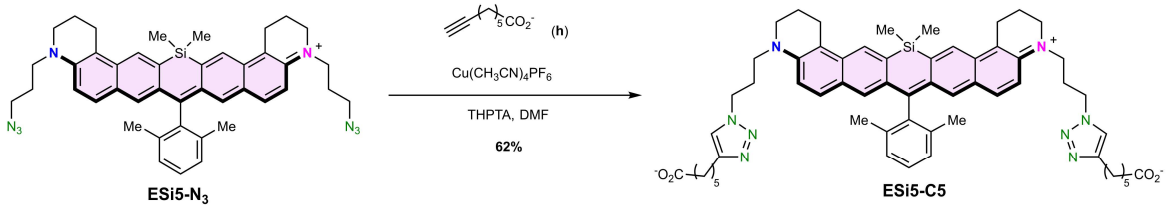

Supplementary Fig. 57: The synthetic scheme of **ESi5-C5**.

Synthesis of **ESi5-C5**: Compound **ESi5-C5** was prepared following the general method with with **h** (purchased from Leyan) in an isolated yield of 62% (43.1mg). ^{1}H NMR (600 MHz, CD_3OD) δ 8.08 (s, 2H), 7.72 (s, 2H), 7.53 (s, 2H), 7.47 (t, J = 7.7 Hz, 1H), 7.37 (d, J = 9.4 Hz, 2H), 7.33 (d, J = 7.7 Hz, 2H), 7.06 (d, J = 9.5 Hz, 2H), 4.48 (t, J = 6.6 Hz, 4H), 3.69 (t, J = 7.3

Hz, 4H), 3.59 (t, J = 5.4 Hz, 4H), 3.10 (t, J = 6.3 Hz, 4H), 2.62 (t, J = 7.5 Hz, 4H), 2.42 – 2.26 (m, 4H), 2.16 – 2.03 (m, 8H), 2.01 (s, 6H), 1.68 – 1.50 (m, 8H), 0.64 (s, 6H). ^{13}C NMR (151 MHz, CD_3OD) δ 183.07, 179.75, 173.00, 153.40, 149.79, 143.76, 139.14, 137.88, 136.67, 136.40, 132.51, 131.25, 130.61, 129.29, 123.85, 117.93, 117.79, 51.70, 51.19, 49.97, 49.40, 39.07, 29.02, 28.50, 27.54, 27.32, 26.51, 24.23, 24.14, 22.37, 20.36, 0.36. HRMS (ESI) (m/z): $[M]^+$ calculated. for $C_{59}H_{71}N_8O_4Si^+$, 983.5363; found: 983.5365.

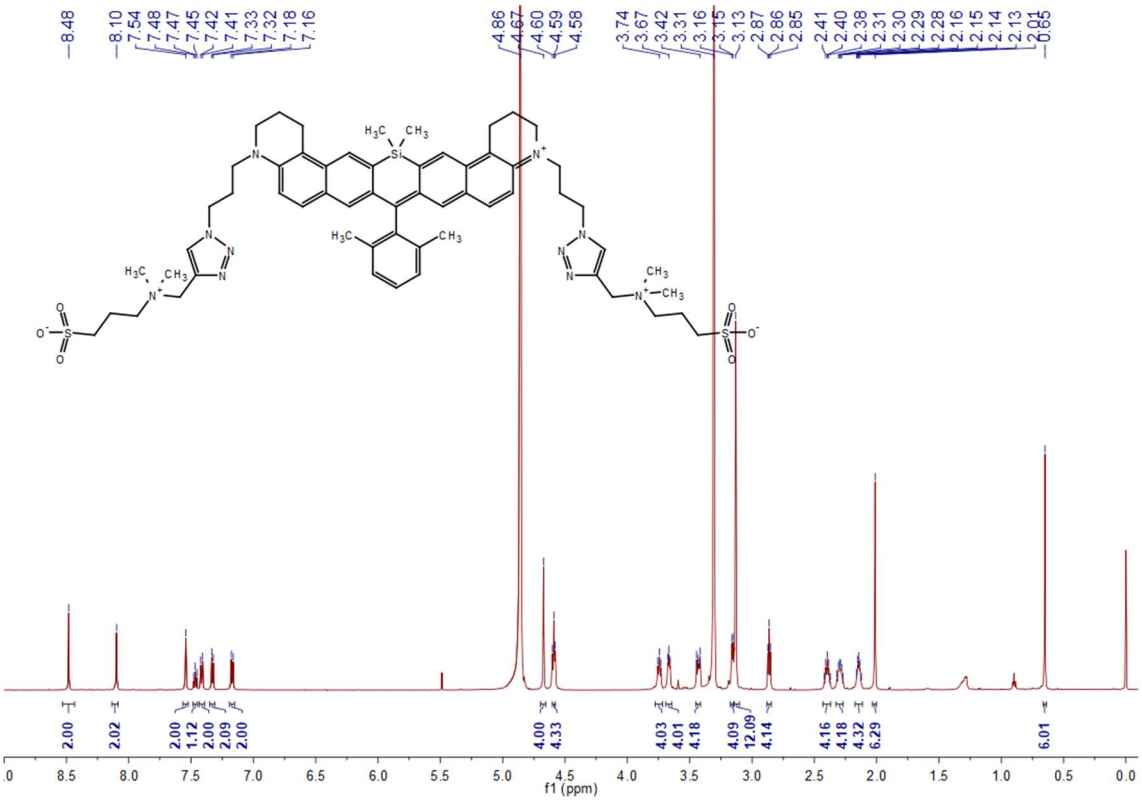

Supplementary Fig. 58: The ^{1}H-NMR of compound **ESi5-NS** in CD_3OD.

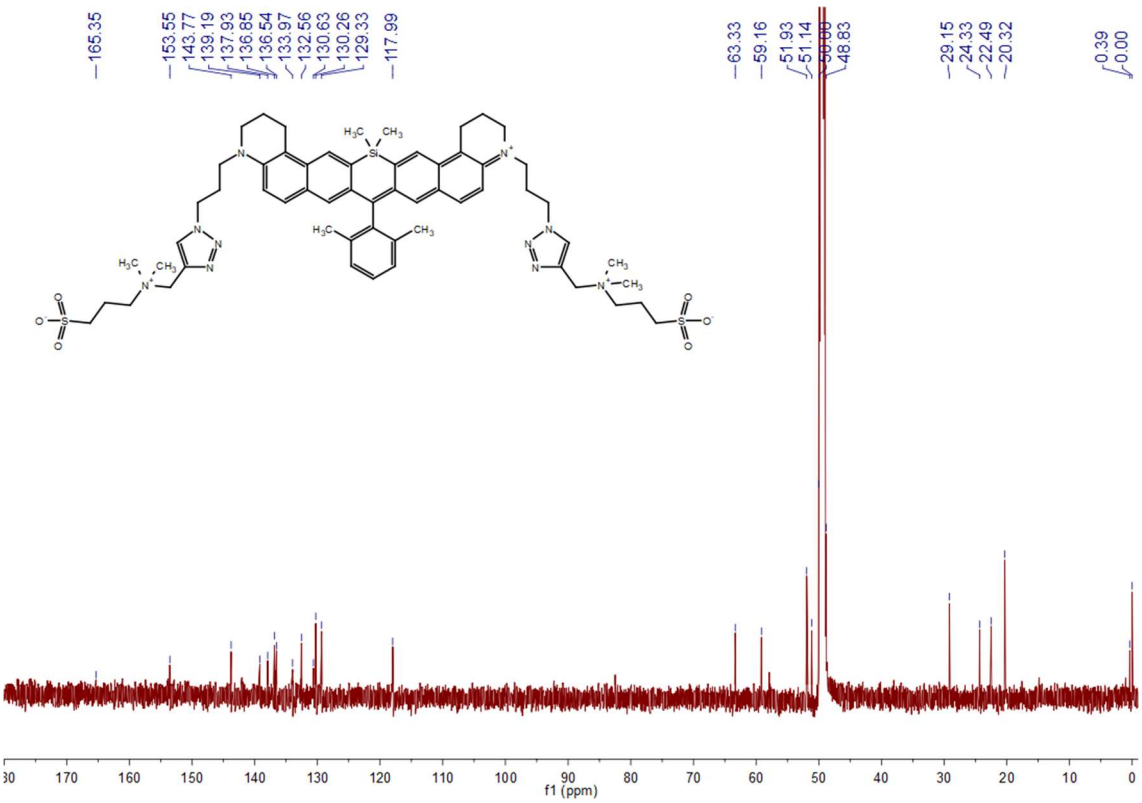

Supplementary Fig. 59: The ^{13}C-NMR of compound **ESi5-NS** in CD_3OD.

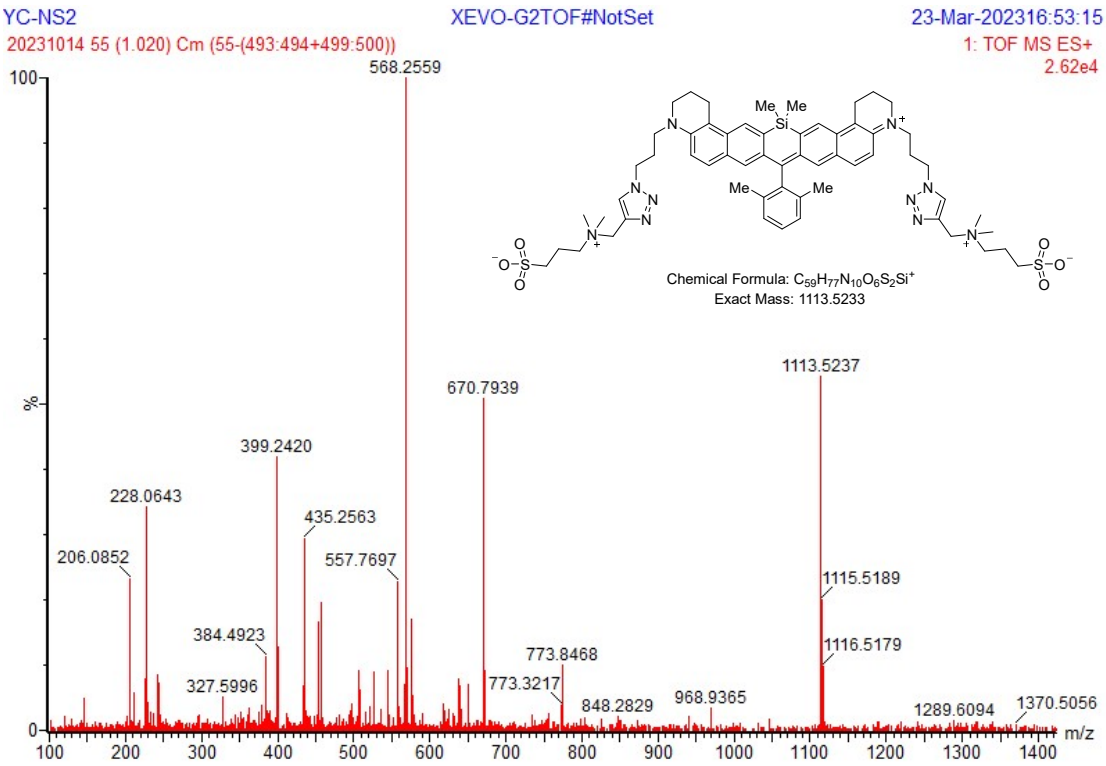

Supplementary Fig. 60: The HRMS of compound **ESi5-NS**.

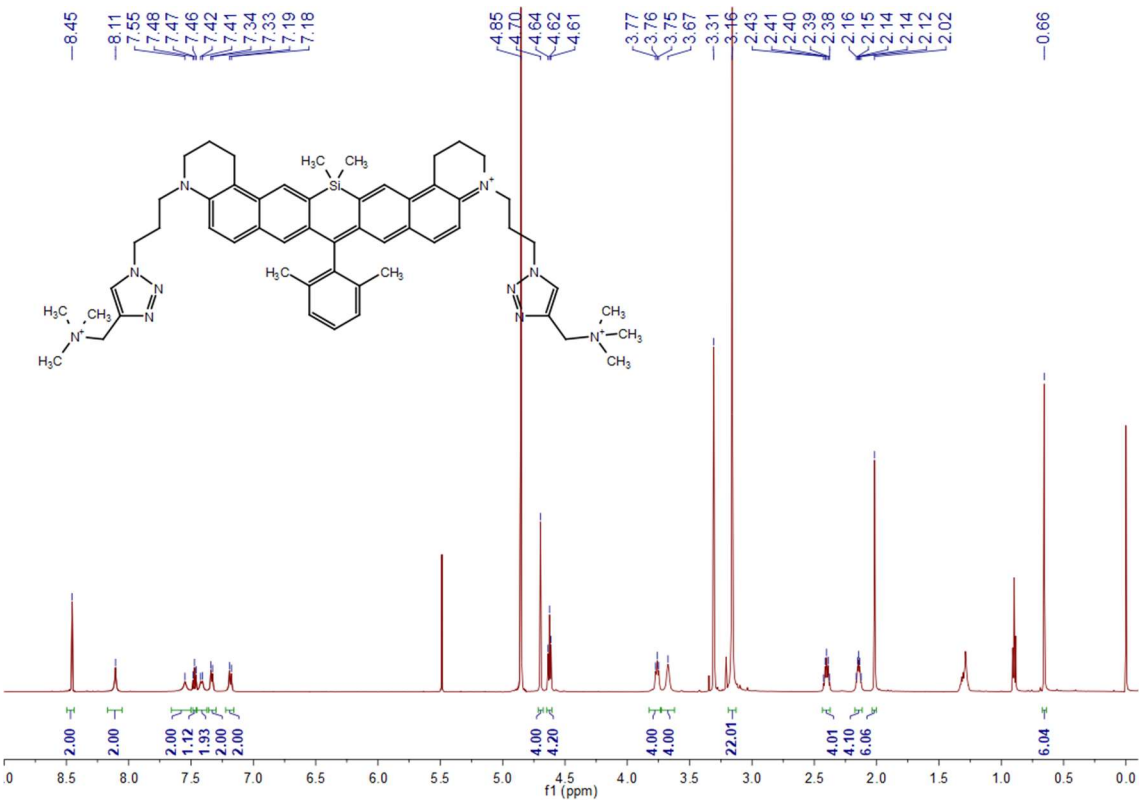

Supplementary Fig. 61: The ^{1}H-NMR of compound **ESi5-N** in CD_3OD.

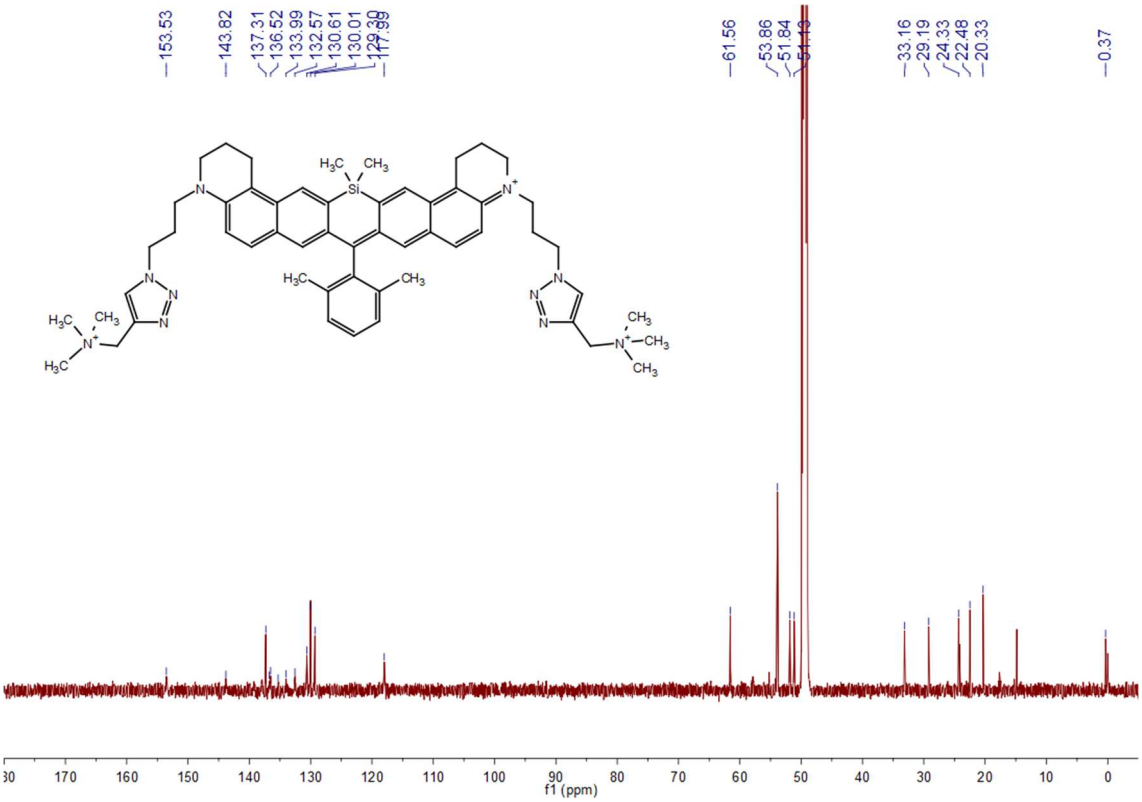

Supplementary Fig. 62: The ^{13}C-NMR of compound **ESi5-N** in CD_3OD

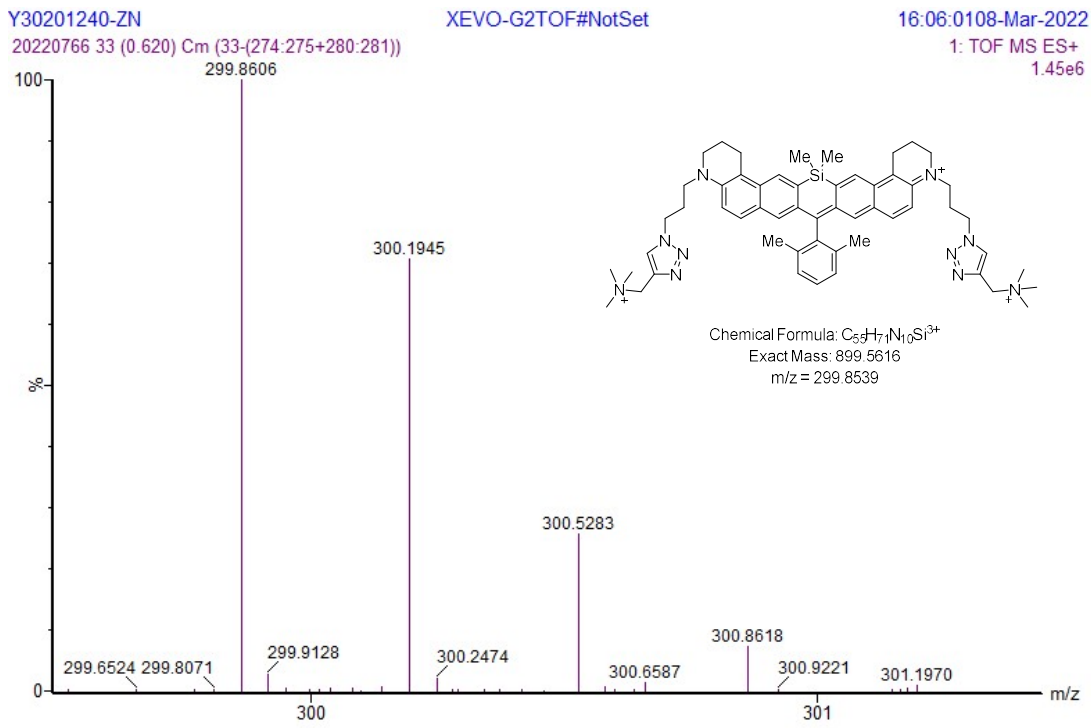

Supplementary Fig. 63: The HRMS of compound **ESi5-N**.

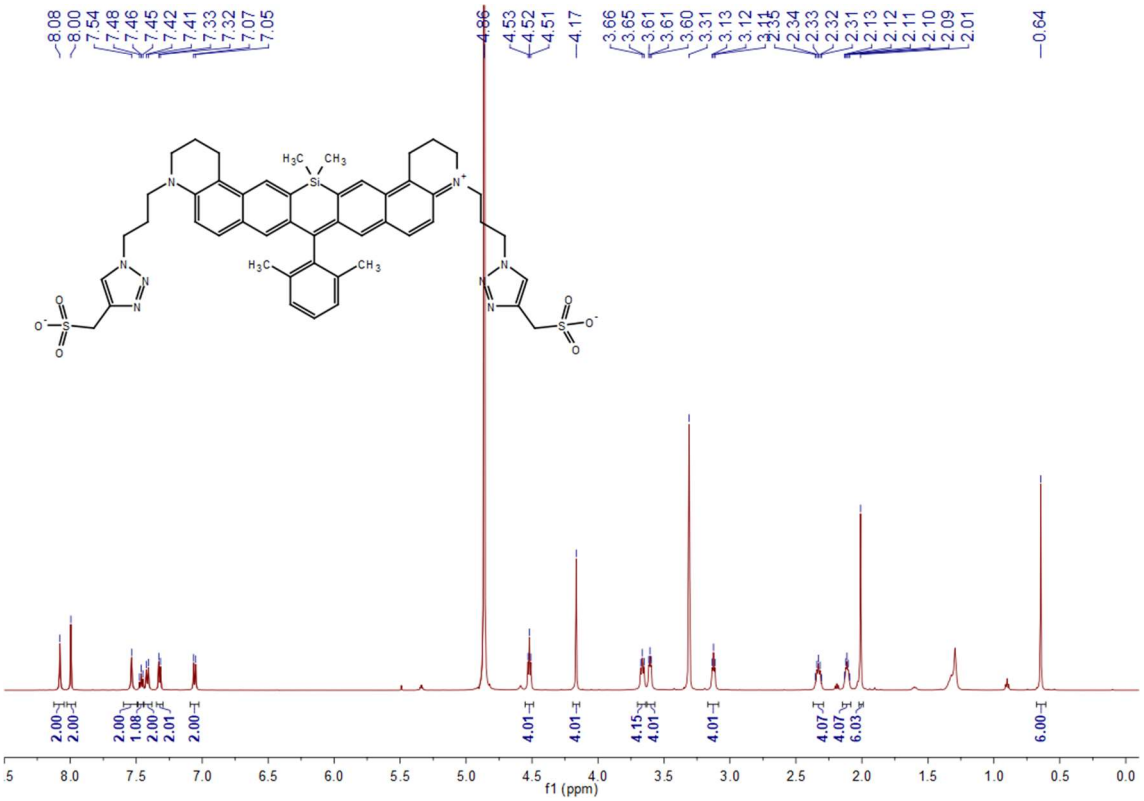

Supplementary Fig. 64: The ^{1}H-NMR of compound **ESi5-S** in CD_3OD.

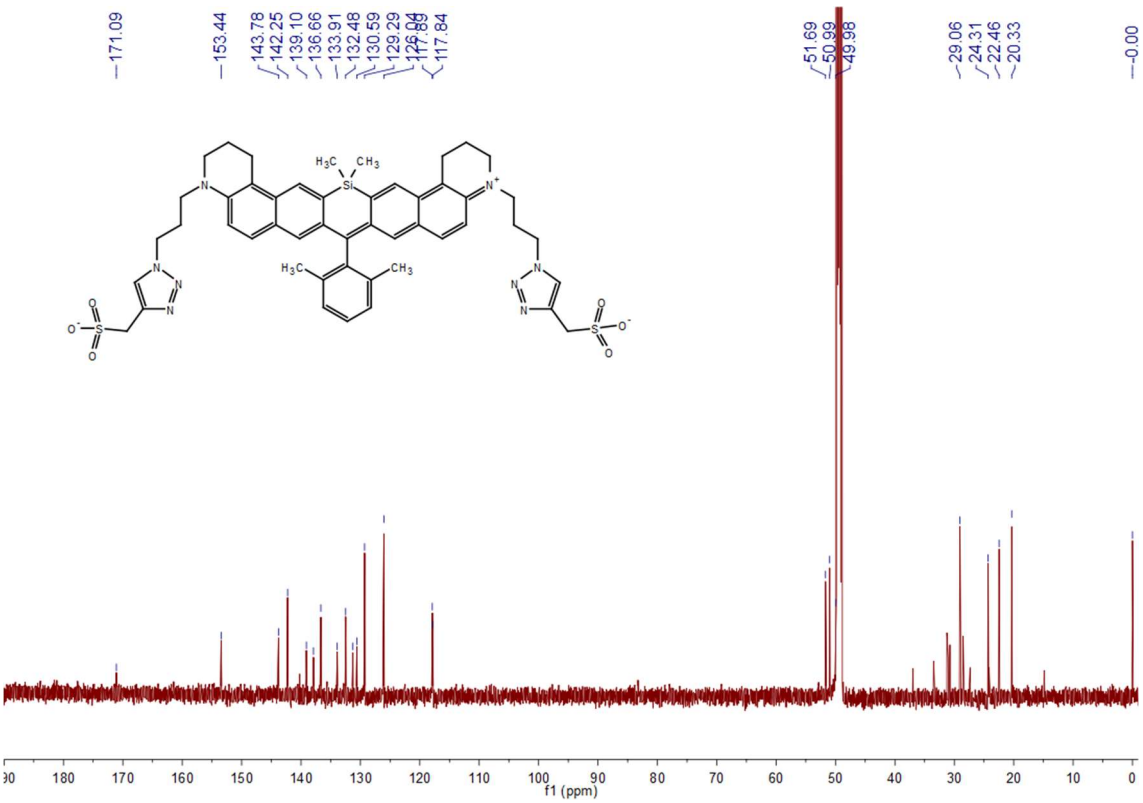

Supplementary Fig. 65: The ^{13}C-NMR of compound **ESi5-S** in CD_3OD.

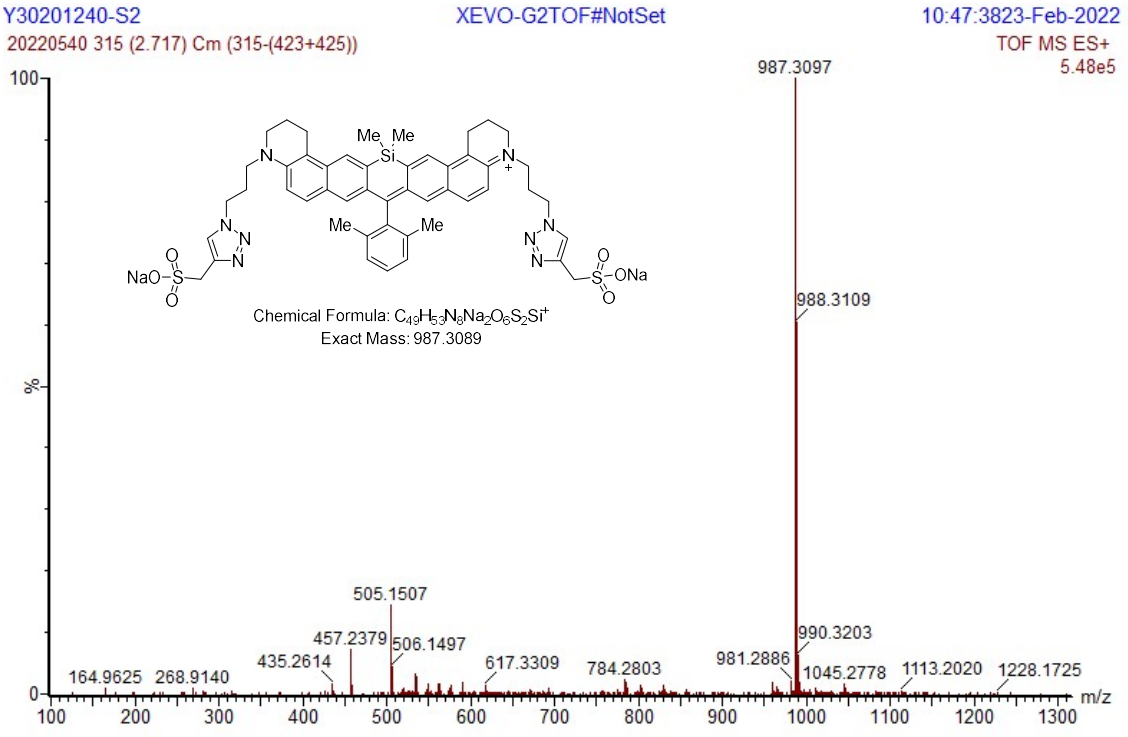

Supplementary Fig. 66: The HRMS of compound **ESi5-S**.

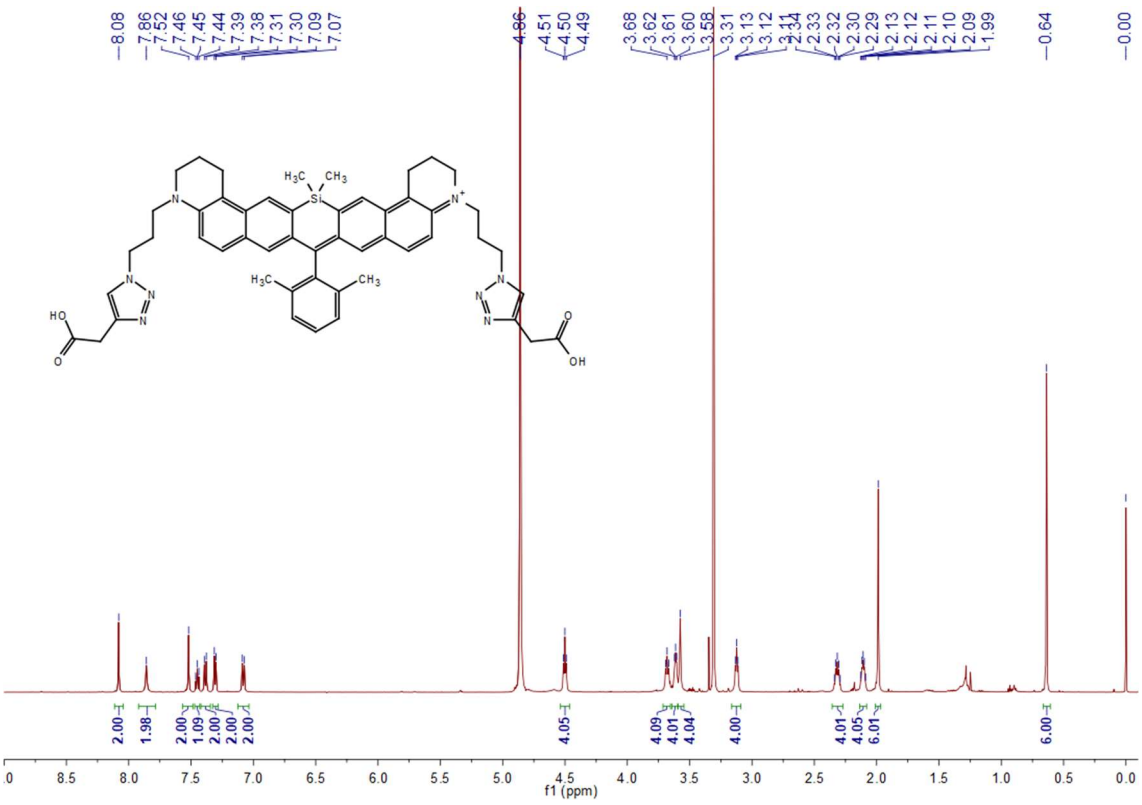

Supplementary Fig. 67: The ^{1}H-NMR of compound **ESi5-C1** in CD_3OD.

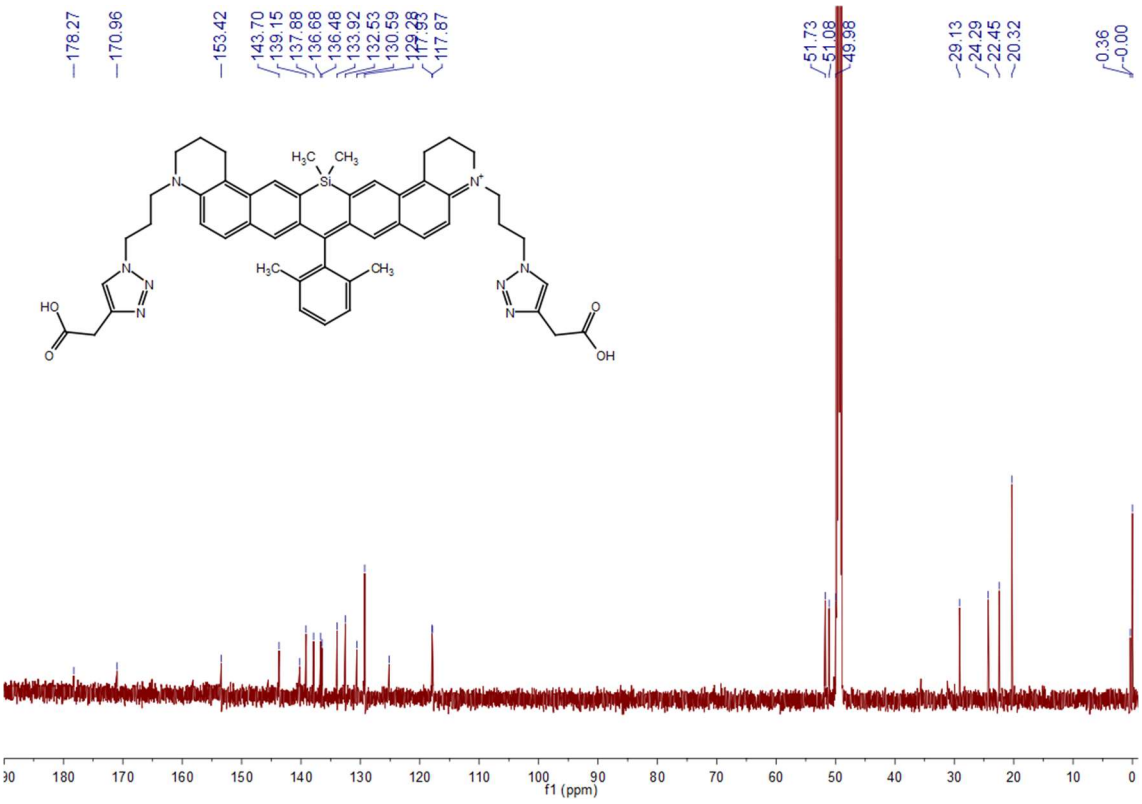

Supplementary Fig. 68: The ^{13}C-NMR of compound **ESi5-C1** in CD_3OD.

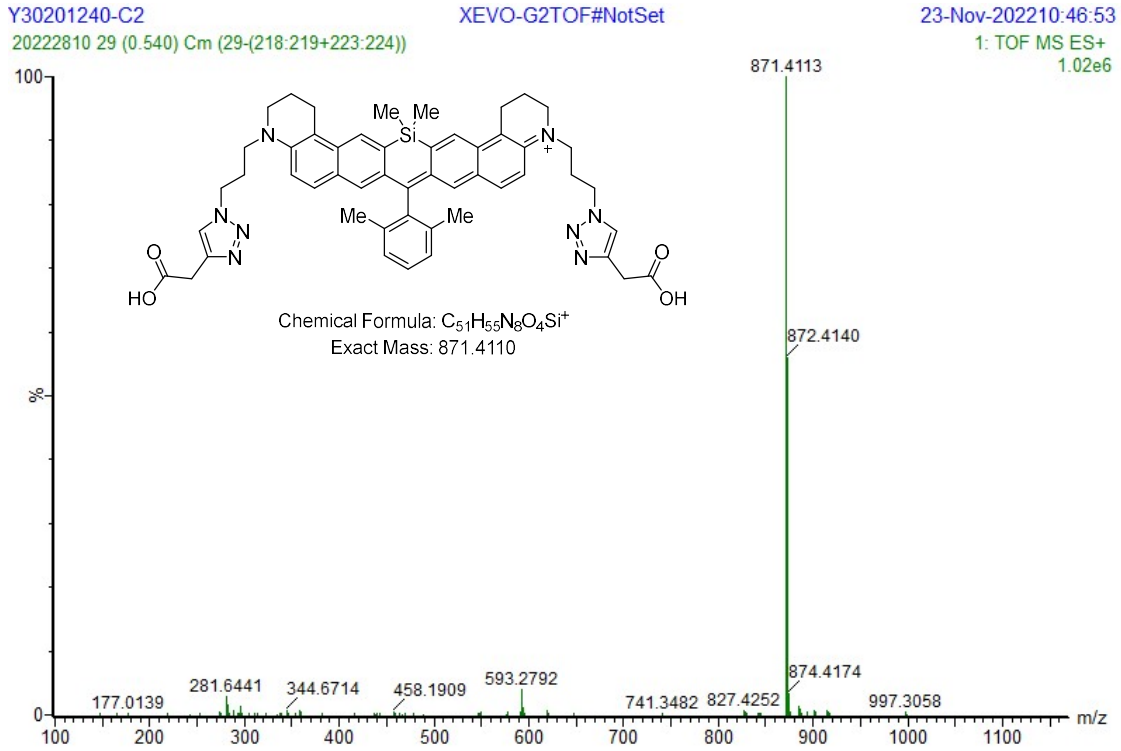

Supplementary Fig. 69: The HRMS of compound **ESi5-C1**.

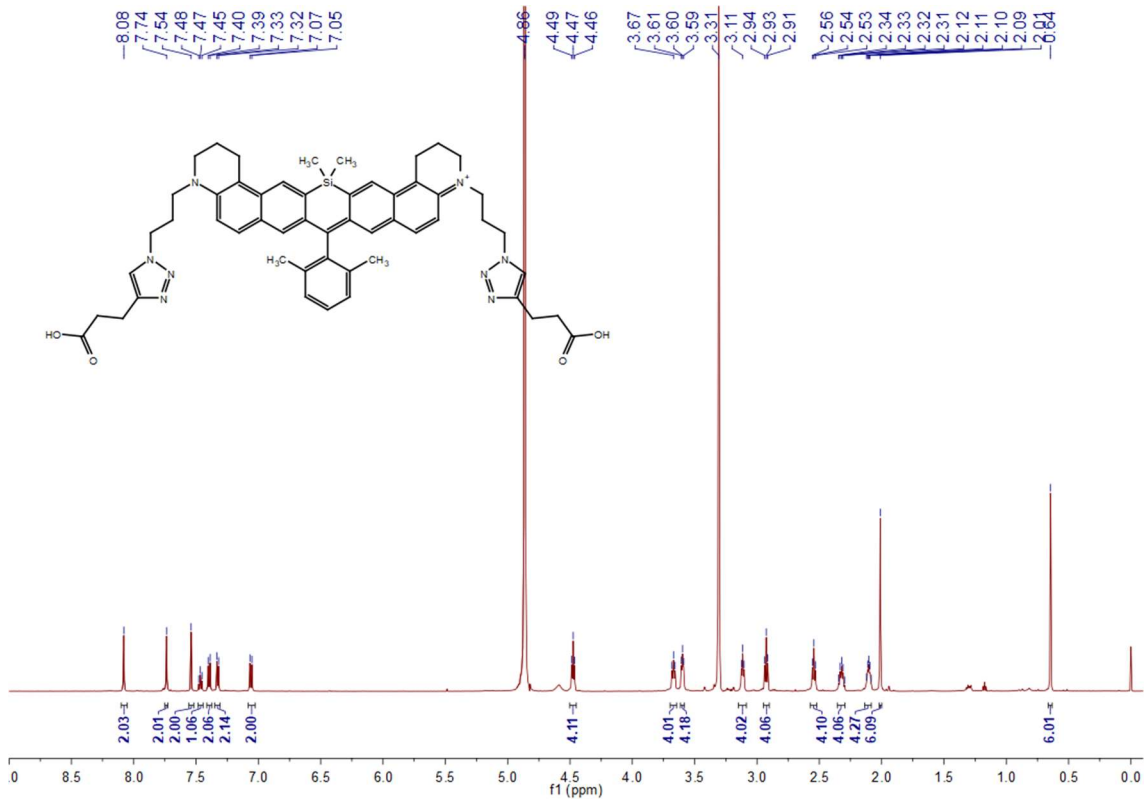

Supplementary Fig. 70: The ^{1}H-NMR of compound **ESi5-C2** in CD_3OD.

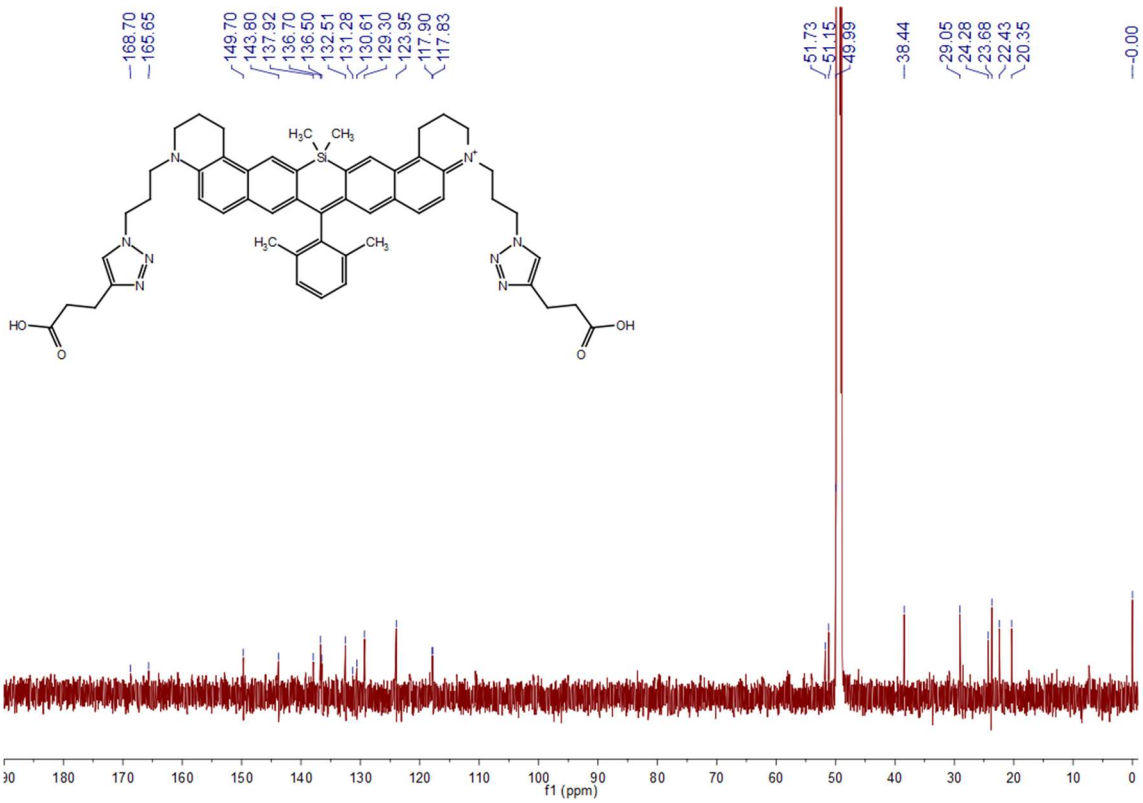

Supplementary Fig. 71: The ^{13}C-NMR of compound **ESi5-C2** in CD_3OD.

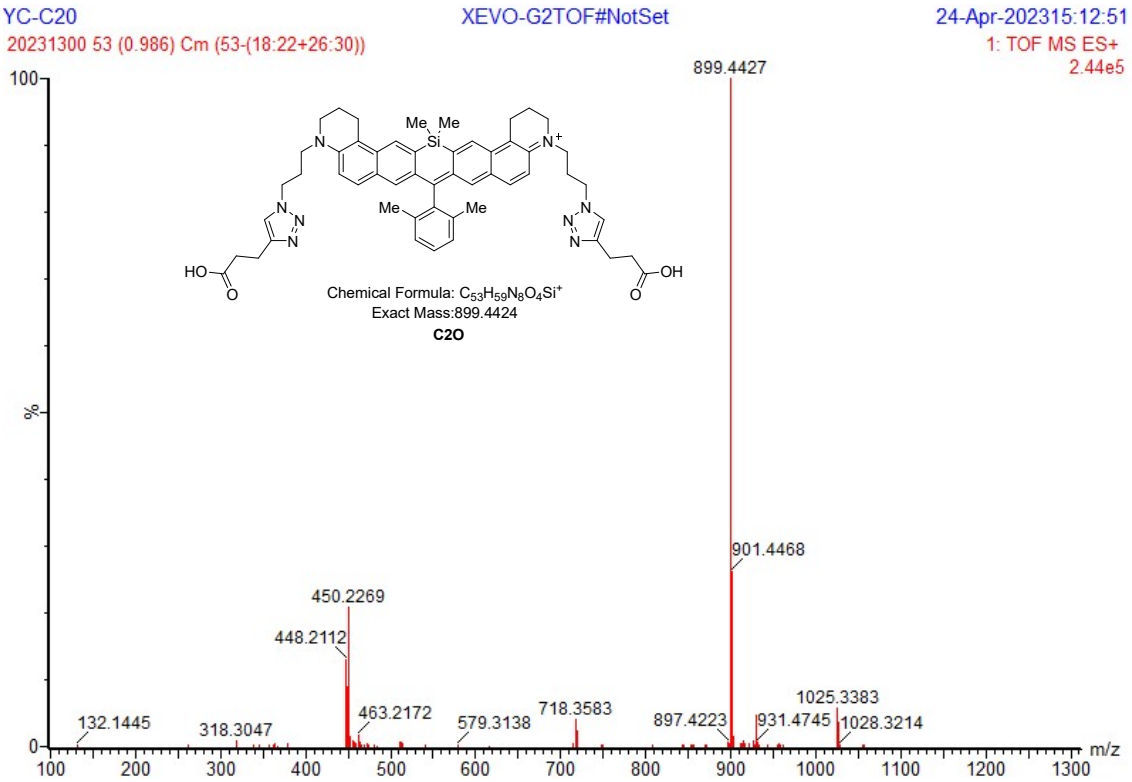

Supplementary Fig. 72: The HRMS of compound **ESi5-C2**.

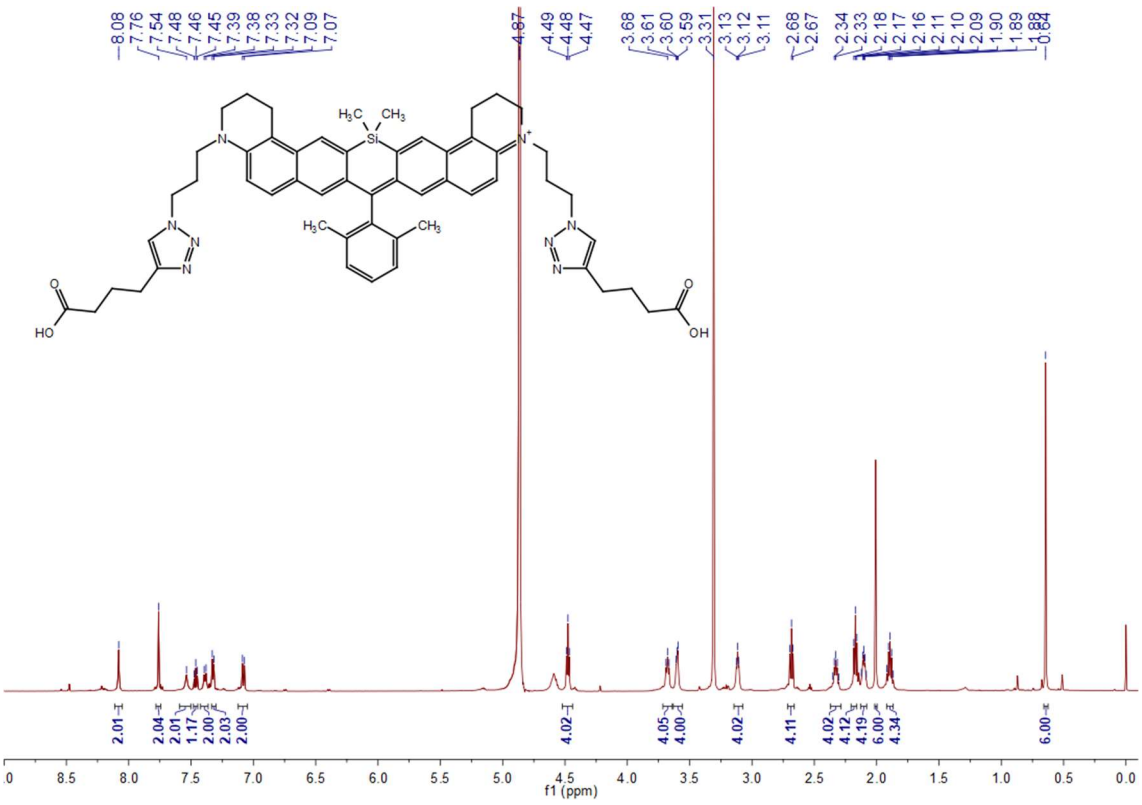

Supplementary Fig. 73: The ^{1}H-NMR of compound **ESi5-C3** in CD_3OD

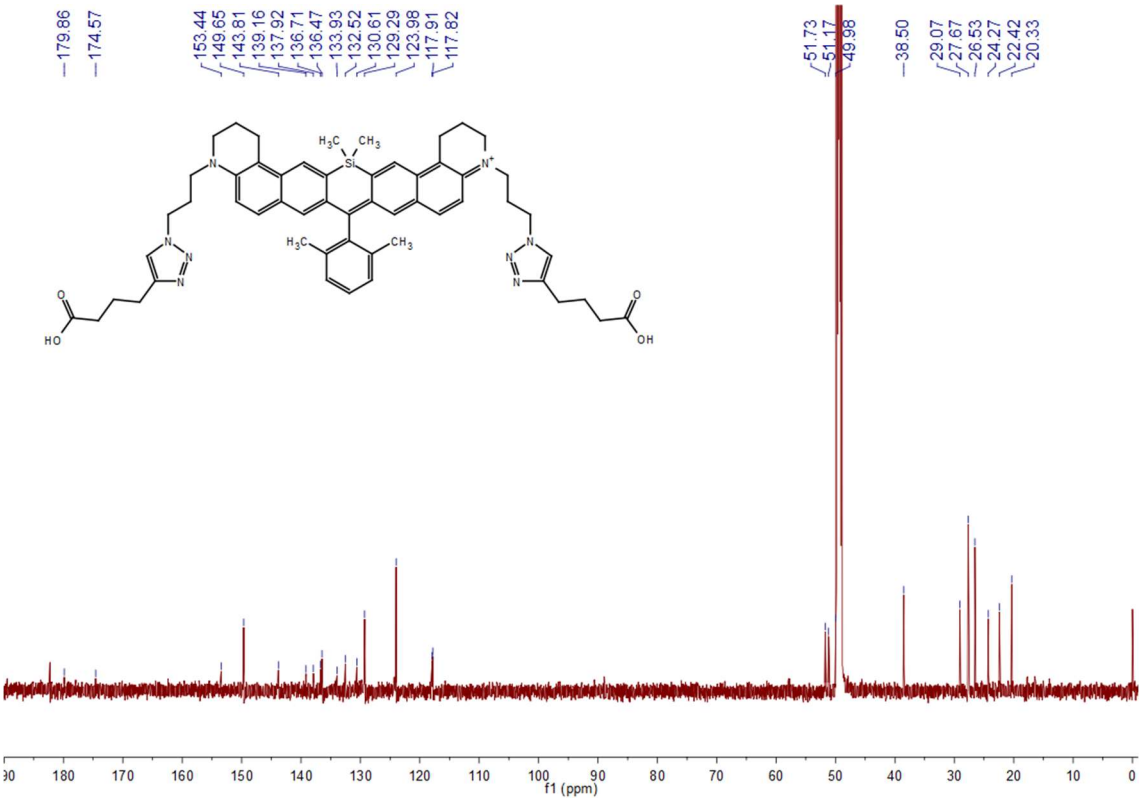

Supplementary Fig. 74: The ^{13}C-NMR of compound **ESi5-C3** in CD_3OD

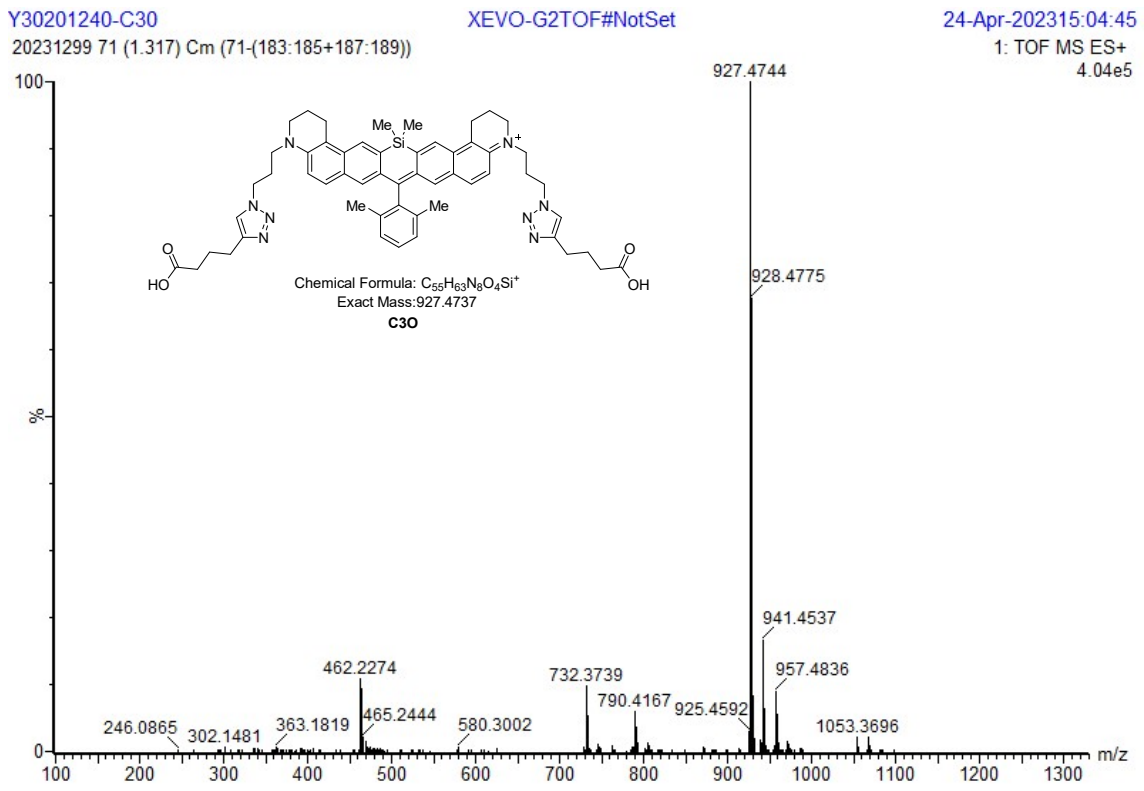

Supplementary Fig. 75: The HRMS of compound **ESi5-C3**.

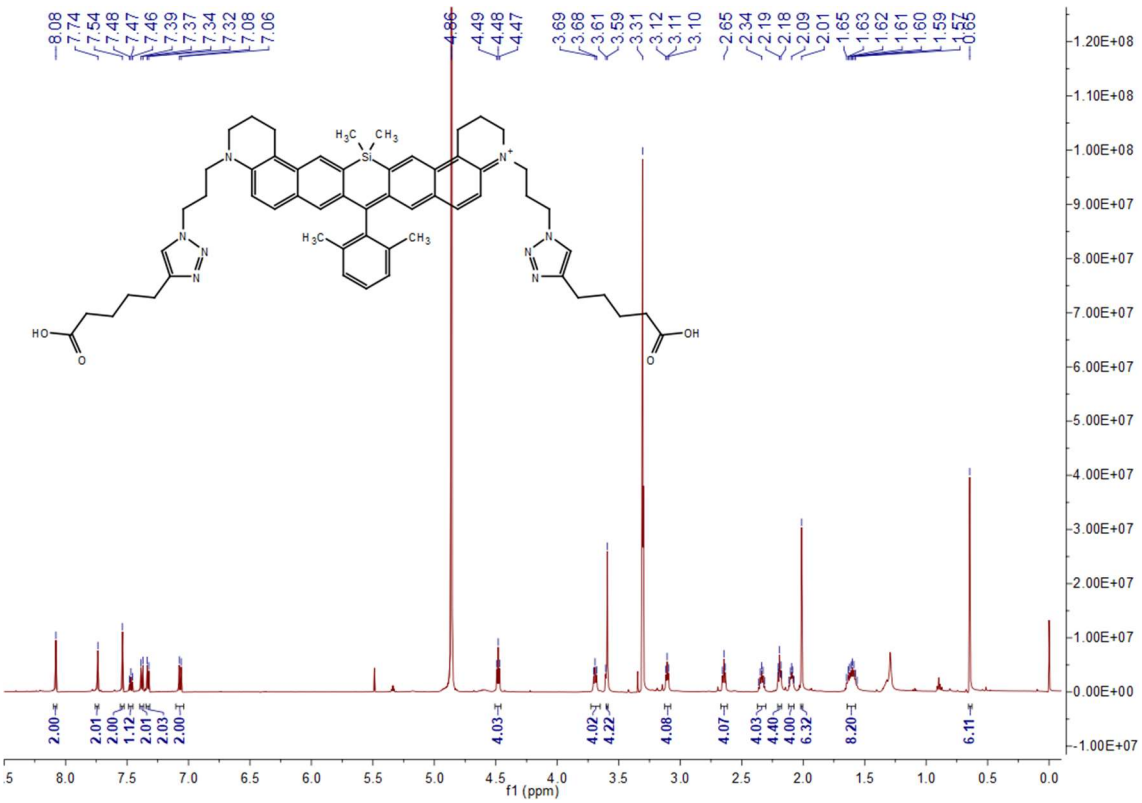

Supplementary Fig. 76: The ^{1}H-NMR of compound **ESi5-C4** in CD_3OD.

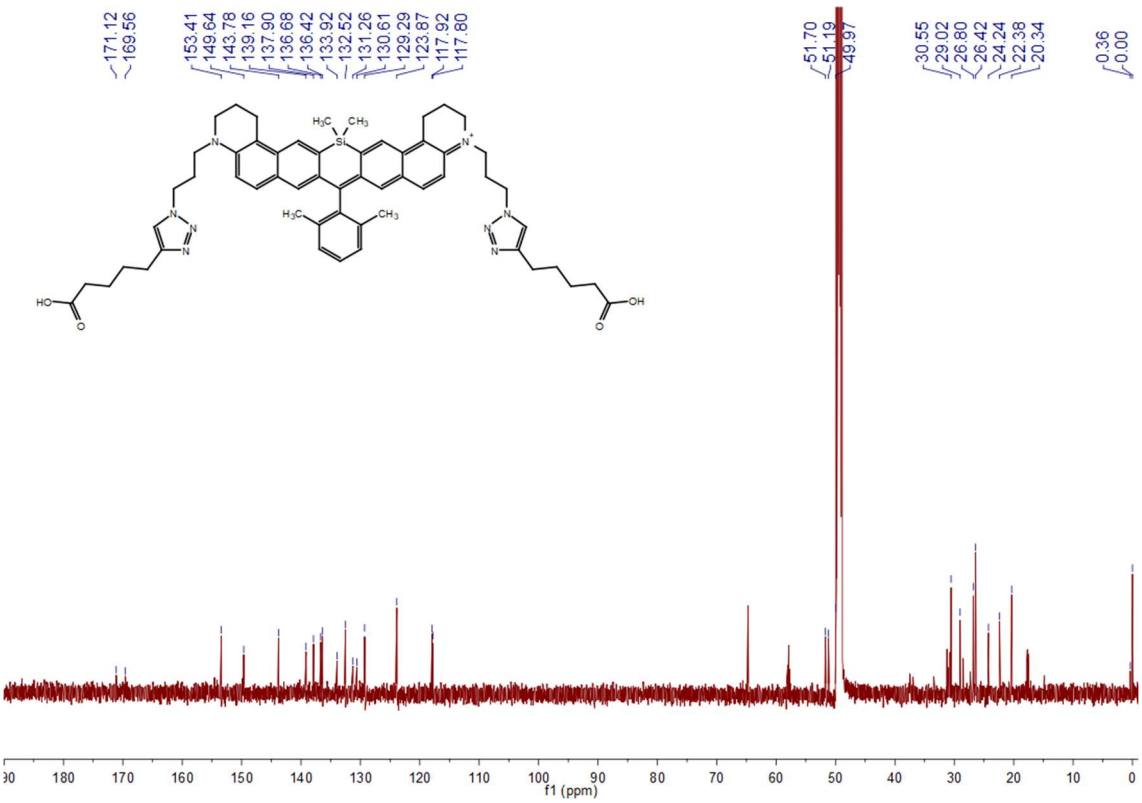

Supplementary Fig. 77: The ^{13}C-NMR of compound **ESi5-C4** in CD_3OD.

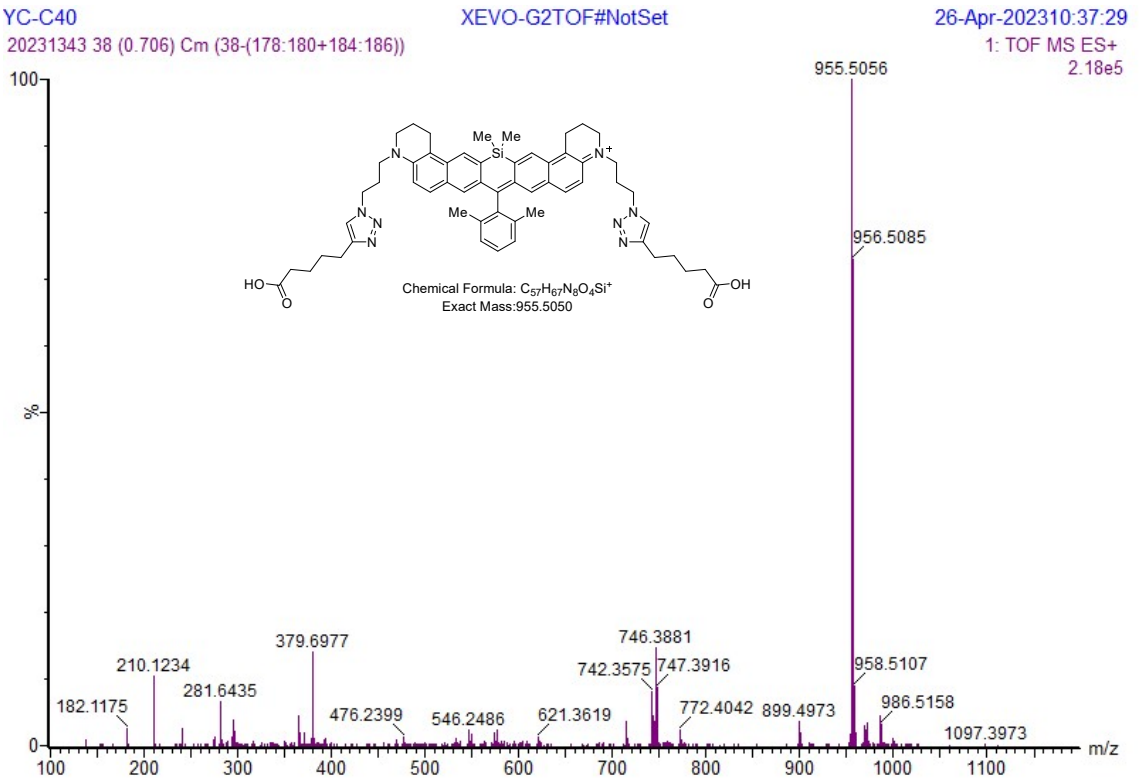

Supplementary Fig. 78: The HRMS of compound **ESi5-C4**.

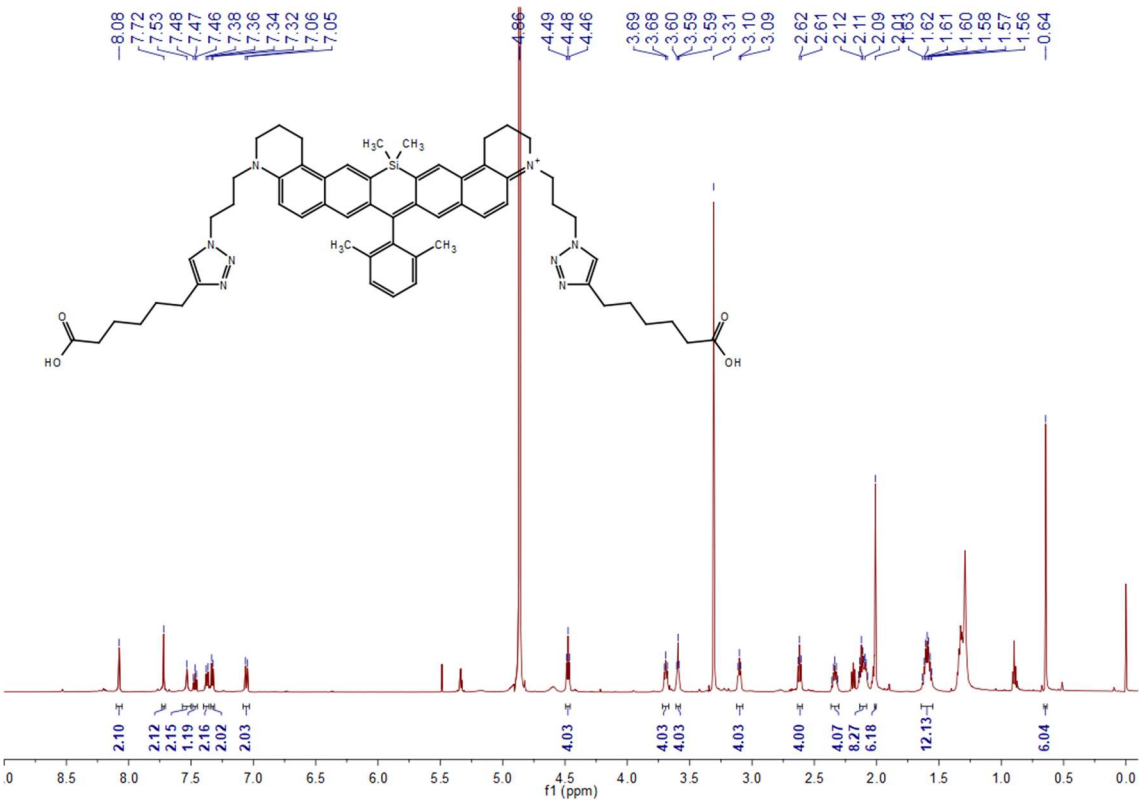

Supplementary Fig. 79: The ^{1}H-NMR of compound **ESi5-C5** in CD_3OD.

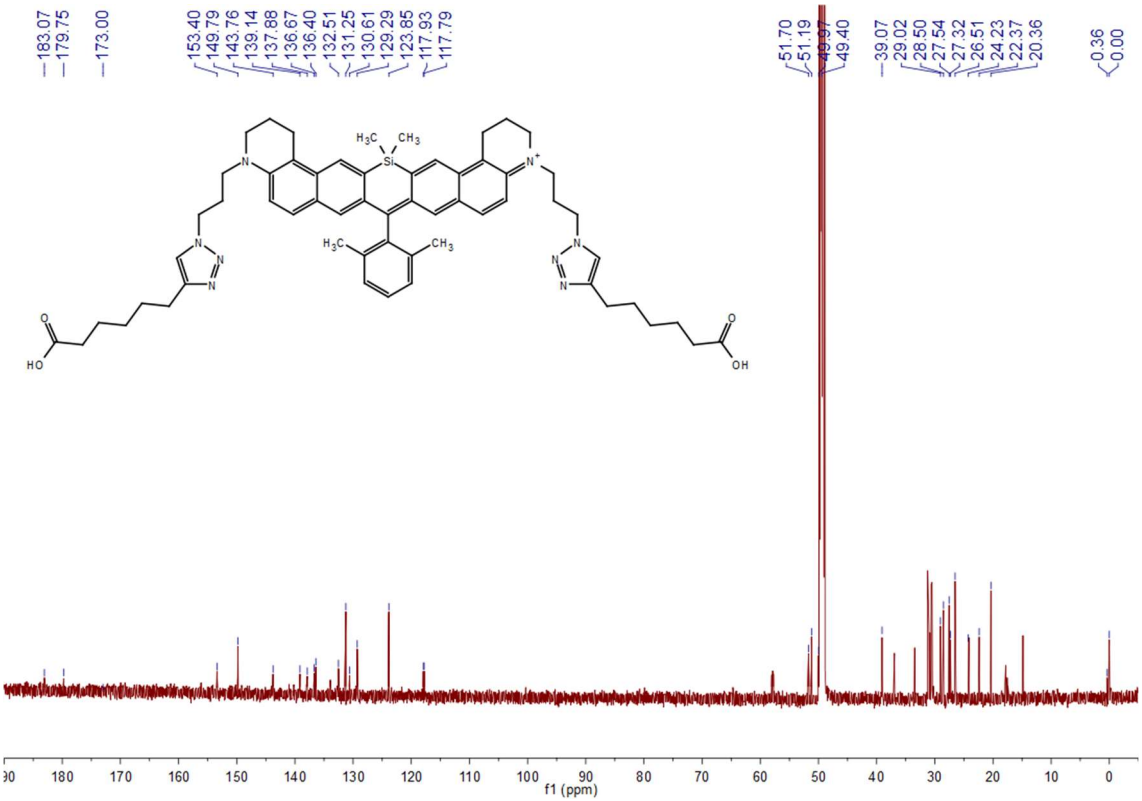

Supplementary Fig. 80: The ^{13}C-NMR of compound **ESi5-C5** in CD_3OD.

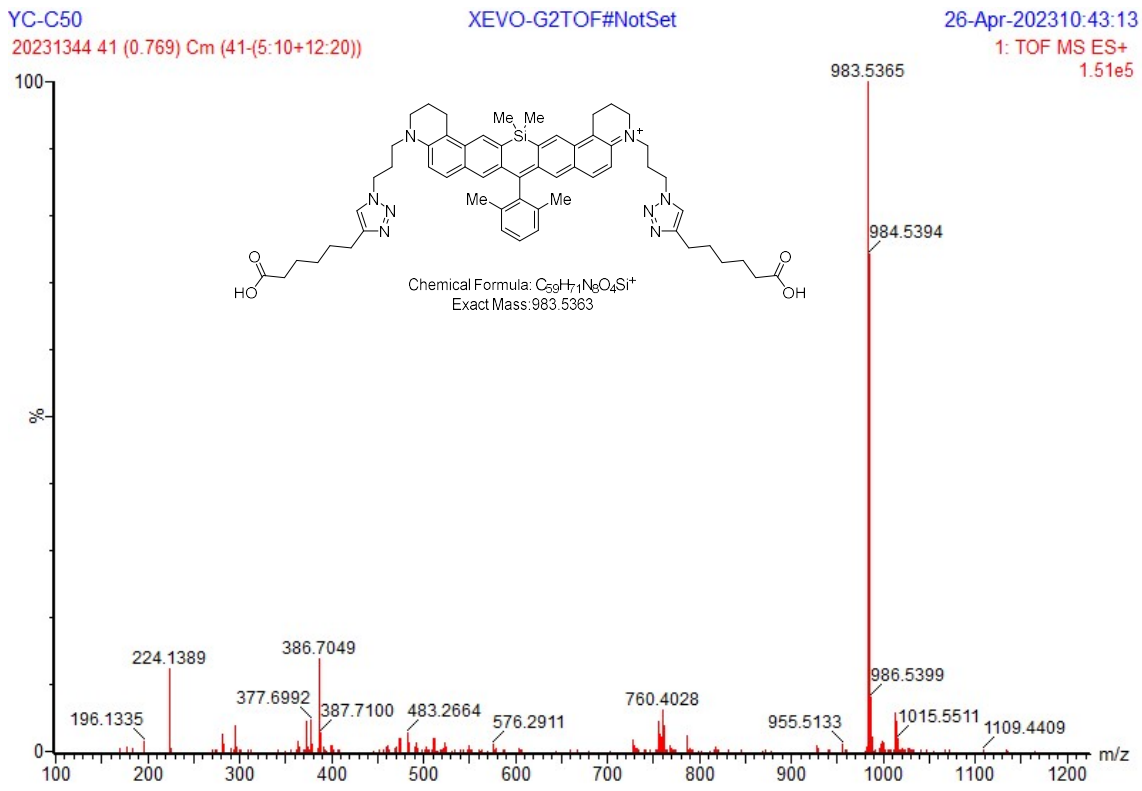

Supplementary Fig. 81: The HRMS of compound **ESi5-C5**.

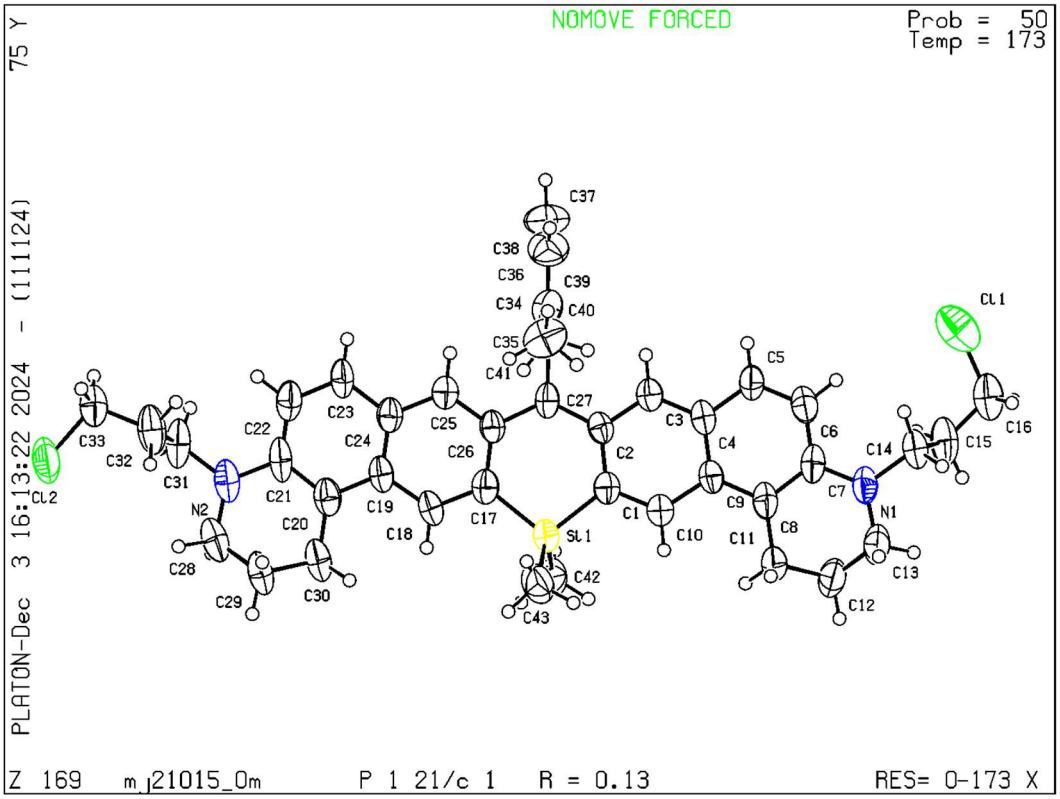

Supplementary Fig. 82: The ORTEP-style illustration of **ESi5•Cl**$^{-}$ (CCDC 2120399).

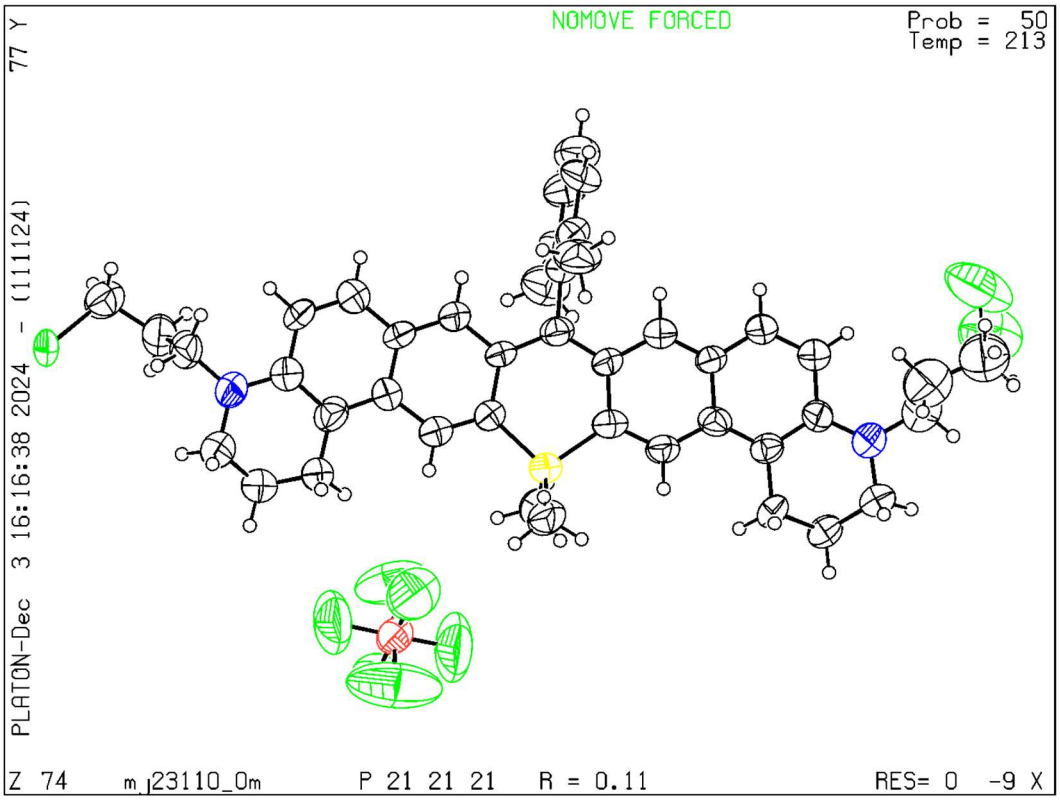

Supplementary Fig. 83: The ORTEP-style illustration of **ESi5•PF_6^-** (CCDC 2364282). (A level b error is indicated for 2364282.)